TAMPEREEN TEKNILLINEN YLIOPISTO
TAMPERE UNIVERSITY OF TECHNOLOGY

**JARKKO PERÄLÄ**

# VIBRATION DAMPING IN MOBILE MACHINES USING PRESSURE FEEDBACK

Master of Science thesis

Examiner: Prof. Reza Ghabcheloo
Examiner and topic approved by the
Faculty Council of the Faculty of
Engineering Sciences
on 4th January 2017

# ABSTRACT

**JARKKO PERÄLÄ**: Vibration damping in mobile machines using pressure feedback
Tampere University of Technology
Master of Science thesis, 66 pages
December 2017
Master's Degree Programme in Automation Technology
Major: Machine Automation
Examiner: Prof. Reza Ghabcheloo
Keywords: Load pressure, feedback control, mobile machine, wheel loader, vibration damping

In this thesis a hydraulically driven wheel loader, which has a flexible crane mounted in front of the machine, has been under research. Flexible boom was excited with a operator given commands, which caused the system vibrate due to different sources of flexibility. The goal was to test cylinder load pressure as a estimate of boom vibrations and use it as a feedback signal to suppress the system oscillations. Therefore, a simulation of wheel loader was created, which replicates real four wheel loader located at the facilities of Laboratory of Automation and Hydraulics.

The first simulator represents a traditional hydraulical system, which has proportional directional valves and variable displacement pump with load sensing functions. A simple controller with pressure feedback vibration damping was designed and tested with different scenarios. After promising results, another simulator was created, which emulates the existing wheel loader better. This experimental wheel loader, called as IHA-machine, has different directional valves and pump operating principal. For working hydraulics, a digital flow control unit was installed. As a power source, IHA-machine has a variable displacement pump-motor, which has a possibility to collect energy from hydraulic system.

Updated simulation version was tested with a controller, which was able to control flow and supply pressure. Vibration damping was added to the flow controller and tested in simulator. After this, the same controller was also tested in real IHA-machine. The results showed, that load pressure as an estimate of system vibrations is a promising way to damping the oscillations that exist in the application. However, the simulation results couldn't be repeated at the same level in the real machine. The control of boom with flow in digital valve environment appeared to be a difficult task when vibration damping was implemented. Regardless, some oscillation canceling was still achieved.

# TIIVISTELMÄ

**JARKKO PERÄLÄ**: Liikkuvien työkoneiden värähtelyn vaimennus painetakaisinkytkennällä
Tampereen teknillinen yliopisto
Diplomityö, 66 sivua
joulukuu 2017
Automaatiotekniikan koulutusohjelma
Pääaine: Koneautomaatio
Tarkastajat: Prof. Reza Ghabcheloo
Avainsanat: Kuormanpaine, takaisinkytketty säätö, liikkuva työkone, pyöräkuormaaja, värähtelyn vaimennus

Tässä diplomityössä tarkastellaan hydraulista pyöräkuormaajaa, jonka eteen on liitetty joustava puomi. Kuormaajan käyttäjä ajoi puomia, mikä aiheutti järjestelmässä erilähteisiä värähtelyjä. Työn päämääränä oli arvioida puomin heiluntaa sylinterin kuormanpainetta hyväksi käyttäen, mitä käytettiin säätimessä takaisinkytkentänä. Testausta varten laadittiin simulaattori, joka vastasi Automaation ja Hydrauliikan laboratorion tiloista löytyvää pyöräkuormaajaa.

Ensimmäinen laadittu simulaattori edusti perinteistä hydraulista järjestelmää, jossa on proportionaali suuntaventtiilit ja säädettävätilavuuksinen pumppu kuormantunto ominaisuuksilla. Tätä varten suunniteltiin yksinkertainen kuormanpainetakaisinkytketty säädin, jota testattiin useassa erilaisessa tilanteessa. Lupaavien tulosten myötä, simulaattoria muutettiin siten, että se vastasi paremmin oikeaa, kokeellista IHA-koneeksi kutsuttua pyöräkuormaajaa. Tämän työhydrauliikkaa ajetaan digitaalisilla virtauksen ohjaus yksiköillä ja säädettävätilavuuksisella pumppu-moottorilla, jolla energian takaisinsyöttäminen on mahdollista.

Päivitettyä simulaattoria testattiin uudella säätimellä, jolla työhydrauliikan virtaus ja syöttöpainetta säädetään. Virtaussäätöön lisättiin värähtelyn vaimennus ja saatua säädintä testattiin simulaattorissa ja oikeassa järjestelmässä. Simulaattorista saadut tulokset osoittivat, että kuormanpainetakaisinkytkentä mukaili hyvin järjestelmän värähtelyjä. Näin ollen se voisi vaimentaa koneen heiluntaa. Tästä huolimatta saman tasoisia tuloksia ei saatu oikeasta järjestelmästä. Puomin ohjaaminen oli vaikea tehtävä virtauksen ja digitaalisten venttilien yhteistoiminnalla, kun värähtelyn vaimennus oli lisätty säätimeen. Tästä huolimatta osa värähtelyistä pystyttiin vaimentamaan.

# PREFACE

This master's thesis was conducte as a part of research project at the Laboratory of Automation and Hydraulics (AUT) in Tampere University of Technology (TUT).

I would like to thank my supervisor and examiner Prof. Reza Ghabcheloo for this wonderful opportunity to work with this challenging task in a supportive working environment. Thanks to Joni Backas ja Ville Ahola for the help and knowledge about IHA-machine.

I also would like to thank my family and friends for their unrelenting support and understanding during this project. Especially, I want to thank my roommates Tomi and Marko for endless entertainment and all the good times.

Tampere, 21.11.2017

Jarkko Perälä

# TABLE OF CONTENTS

# LIST OF ABBREVIATIONS AND SYMBOLS

| | |
|---|---|
| AMM | Assumed Modes Method |
| BEM | Boundary Element Method |
| CAN | Controller Area Network |
| DFCU | Digital Flow Control Unit |
| PID | Proportional Integral Derivative |
| DIO | Digital Input Output |
| DRG | Electrical load sensing |
| FEM | Finite Element Method |
| FIR | Finite Impulse Response |
| GBE | Generalized Beam Element |
| GMA | Geometric Moving Average |
| GPI | Generalized Proportional Integrator |
| IMU | Inertia Measurement Unit |
| IRC | Integral Resonant Control |
| LS | Load Sensing |
| NPF | Negative Position Feedback |
| PZT | Lead Zirconate Titanate |
| PPF | Positive Position Feedback |
| RTI | Real Time Interface |
| VDC | Virtual Decomposition Control |

| | |
|---|---|
| $A$ | general area |
| $B$ | system bulk modulus |
| $B_h$ | hose bulk modulus |
| $B_0$ | oil bulk modulus |
| $E$ | Young's modulus |
| $F$ | generalized forces |
| $f$ | generalized force of the joint |
| $F_c$ | Coulomb sliding force |
| $F_f$ | friction force |
| $F_s$ | maximal static friction force |
| $I$ | moment of inertia |
| $I_{zz}$ | area moment of inertia |
| $J$ | Jacobian matrix |
| $K$ | generalized stiffness matrix |
| $k$ | spring constant |

| | |
|---|---|
| $k_{P_L}$ | pressure feedback gain |
| $k_{tanh}$ | tanh tuning parameter |
| $k_v$ | viscous friction coefficient |
| $k_{vib}$ | vibration gain |
| $L$ | length of beam |
| $l$ | length of a single GBE |
| $M$ | mass of beam |
| $m$ | mass of a single GBE |
| $n$ | rotation speed |
| $n_{vol}$ | volumetric efficiency |
| $P$ | force at the free end of GBE |
| $p$ | fluid pressure |
| $p_A$ | cylinder A chamber pressure |
| $p_B$ | cylinder B chamber pressure |
| $P_L$ | load pressure |
| $Q$ | fluid flow |
| $Q_{cmd}$ | displacement command signal |
| $Q_{meas}$ | measured pump displacement |
| $Q_{ref}$ | desired pump displacement |
| $S$ | vertical deflection at the free end of GBE |
| $T$ | moment at the free end of GBE |
| $u$ | reference signal |
| $V$ | system volume |
| $v$ | sliding speed |
| $V_h$ | hose volume |
| $V_k$ | displacement per revolution |
| $v_s$ | sliding speed coefficient |
| $V_0$ | cylinder dead volume |
| $X$ | generalized coordinates |
| $x$ | general position |
| $x_{ref}$ | reference position |
| $\alpha_{gma}$ | GMA filter parameter |
| $\theta$ | slope respect to the free end of GBE |
| $\lambda$ | piston area ratio |
| $\omega_c$ | controller bandwidth |
| $\tau$ | joint torque |

# 1. INTRODUCTION

Vibration is very common feature, when dealing with mobile machines. The first structural oscillations appear when the diesel engine is started and pistons are moving the piston chambers. The moment when machine starts to move on the ground, arouse vibration as well as driving on the bumpy road. Manipulators in the mobile machines create structural vibrations, especially when handling heavy loads, which can be logs, containers or flowing concrete.

The urge for better energy efficiency creates a need for lighter machine structures. The improvements in materials create smaller and thinner bodies for frames and beams, while remaining as strong as before. This evolution comes with the cost of increased structural bending and beam oscillation.

The research area of flexible manipulators has grown greatly over few decades. Majority of these experiments are on the field of robotics, that are researching systems usually driven by electrical motor. Experiments often include testing controllers or modeling methods, while hydraulics systems remaining as a niche field, but some experiments can also be found on that particular area.

Hydraulically operated systems generate forces using fluid pressure in the actuators. When manipulator beam starts bending, it affects to cylinder by generating force, which is parallel to the bending direction. When the force changes, the pressure inside the cylinder changes also. This means, that measuring the pressure inside cylinder and recording the variations in it leads a good approximation of the beam bending. This is the core idea this thesis is build on.

Flexible manipulators have been researched a long time and the field keeps growing. In this thesis a closer look is taken to this matter. Different kind of modeling and controlling methods are reviewed and discussed. One of the modeling methods is chosen, inspected closely and then utilized to create a model of a flexible beam.

Since the emphasis was put on mobile machines, a simulation model of a Wille urban wheel loader was created and the flexible link model was added as an auxiliary equipment. Simulation model is based on a real machine, which is located at the Laboratory

of Automation and Hydraulics and dubbed as IHA-machine, which was also used during real test environment phase.

Controller for the vibration damping is based on previous tests, which included two mass spring damped system and Hiab crane simulation. This controller design is discussed in detail in chapter 6. All the simulation and real machine test results are then presented at the chapter 8. This includes common observations, which can be seen in the figures but also user experienced details.

In the end possible future research topics are presented among some points, which could be improved in this thesis. Lastly, some conclusion are drawn.

# 2. STATE OF THE ART FLEXIBLE BOOM

This chapter is about flexible boom and manipulators, especially modeling and controlling them. These matters draw attention, since this area of research have been under the scope for several years. This section shows that, there are four common ways of modeling flexible manipulators: finite element, boundary element, assumed modes and lumped parameter methods. Instead, the amount of control schemes is quite vast.

This chapter consist of modeling part, controlling part of flexible boom and as a last section sensor systems which are used in flexible manipulators. Control section is divided into two subsections, which are model and nonmodel-based methods respectively. This chapter is based heavily on reference [27], since it is dealing with same subject.

## 2.1 Modeling of flexible boom

Modelling methods generally start with a simple single rigid link manipulator, which stores certain amount of kinetic and potential energy. In the case of flexible links, potential energy is stored into deflections of joints, actuators and drives. In systems, where shafts or belts are acting as drive units, lumped parameter method is often suitable, since these units have relatively low inertia. Torsion of the links stores potential energy and only a little kinetic energy. Since the low mass inertia around the longitudinal axis of the link, this motion can be described as a massless spring. Axial forces in these systems are often storing only a little potential energy due to stiffness, therefore they are often neglected. Bending stores significant amount of potential and kinetic energy, thus good flexible model must include both elements. Euler-Bernoulli beam equation is often used to take bending into account, but it ignores the shearing and rotary inertia effects. Instead, Timoshenkos beam equation take these into consideration, which is a must, when beam is relatively short compared to its diameter. [18]

Assumed Modes Method (AMM) describes the system deformation as truncated finite modal series, in terms of spatial mode eigen functions and time varying mode amplitudes [18]. AMM uses trial functions and generalized coordinates, which are forming a boundary value problem, which can be described as eigenvalue problem.

Finite Element Method (FEM) is very frequently used modeling method for flexible structures. In complex geometries solving original differential equations in really difficult. This derives the idea of FEM, where complex structures are divided into smaller subproblems. In short, FEM represents the target structure as a collection of elements. There is different types of elements each having pros and cons. For example beam element is allowing both translational and rotational movements at each nodes but represents a constant cross section. Brick or tetrahedra elements are used to model solid objects but the amount of nodes is much higher than in beam type elements [13]. Together these elements form a mesh on geometry. Next step is to convert original differential equation form of the partial differential equation into integral form, which are simpler equations. For stationary problems where coefficients do not depend on the solution or gradient, result is linear system of equations. A case where coefficients do depend on the solution or gradient, the result is a system of nonlinear equations. In time-dependent problems, the result is a set of original differential equations. These equations combined with boundary conditions, a global system of equations can be formed, which represents the entire system. [34]

In book [2], the author claims that Boundary Element Method (BEM) is powerful alternative choice for the FEM. Boundary Element Method discretization is restricted only to the boundaries of the system, where as FEM divides the whole system into smaller pieces. Advantages are driven from computational effectiveness, since the calculations are done only on the system boundaries, where as FEM uses all the nodes mesh grid provides. Therefore BEM is more suitable for control design purposes. Computational effectiveness has been verified also with error estimators and few other applications. On the other hand, BEM loses its computational effectiveness when considering inhomogeneous non-symmetric and nonlinear problems. BEM also needs more knowledge of the system fundamentals compared to the FEM, when simulating the physical model of the system. [2, 48]

Lumped parameter method describes the flexible beam as a series of rigid bodies, which are connected to each other with springs and dampers. This method is easy to implement with Simulink SimMechanics, by creating a series of rigid body parts connected with joints. Coefficients are determined by the material properties and the structure geometry. Lumped parameter modelling method suits well for structures with linear geometries, but it also can be implement into more complex systems, although other methods should be considered in that case. [12] Implementation of lumped parameter method is discussed in chapter 3.

## 2.2 Controlling of flexible boom

Control methods can be generally divided into two major sections; model-based and nonmodel-based control schemes. These are discussed in the text and a table 2.1 has been created for comparison. As known, feedback controlling uses measurement data acquired from the system to adjust the reference input of the system. Feed-forward systems use the knowledge of system, which predicts the system behavior. Therefore the reference input can be modified in order to archive a desired outcome.

### 2.2.1 Model-based control methods

Command shaping technique is one way to damp vibrations in flexible structures. One example is Finite impulse response (FIR) filter, which was designed for mobile harbor luffing crane with hydraulic cylinder shown if figure 2.1. The goal was to filter the command signal given by the crane driver hand lever, to reduce oscillations in the system. In this case FIR filter was easy to design since the designing procedure was based on one nominal frequency. The drawback of the FIR filter was that is delays the hand lever signal by half the period of the designed nominal frequency of the filter. [29]

***Figure 2.1.*** *Liebherr harbor mobile luffing crane. [29]*

Flatness based feed-forward controller is more complex control approach and it needs complete model of the system. In addition, it needs a numerical trajectory generation

out of the hand lever inputs. This control method basically has no delay, but it has few disadvantages, as it requires feedback controller for exact trajectory tracking. [29]

Another model based approach is inverse dynamics model-based control. It utilizes modal analysis, which assumes that the deformations of flexible link can be described as a finite series expansion, which include elementary vibration modes. This method however may result in inaccurate control, since it relies on precise model. [41]

Optimal control /optimal trajectory planning is a way of determining control and state trajectories in order to minimize performance index. The target is to find control law, in a way that desired optimality is achieved. Its advantages are efficient path planning, but it is dependent on system compensation and feedback control if there occurs any disturbance in the system. Therefore small changes or variations in model parameters can diminish the performance of the system. [23]

Another model-based approach uses Virtual Decomposition Control (VDC) in order to control 1-dof hydraulically actuated boom. VDC is subsystem based, nonlinear control method developed for high degrees of freedom assemblies. Tests showed some promising results for hydraulically driven flexible manipulators. Despite relatively good oscillation canceling, parameter acquisition was a challenging task and the accuracy of the system, depended on operation point. [33]

Model-based control schemes aren't reliable control strategy alone, since they often require feedback control to handle external disturbances, variable payload or unmodelled vibration modes. Systems that use both feedback and feed-forward controlling features are usually called as hybrid control methods. These aim pick up the best attributes of each control schemes or counter the weaknesses of other control method.

### 2.2.2 Nonmodel-based control methods

Nonmodel-based control schemes are usually feedback systems, which don't require accurate modelling of the system, hence it fits for the systems which have complex mechanical model or they include unknown parameters. The biggest disadvantage of this method is lag caused by measurement loop.

Positive or negative position feedback (PPF/NPF) is often used in applications where multiple modes of vibration occur. Feedback loop is constructed with displacement sensor and natural frequency is needed to successfully apply this strategy. PPF/NPF has ability to adapt changes in the system, but frequency should not be change. Also situations where multiple frequencies are needed to damp, controller may be difficult to tune. [40, 45, 44]

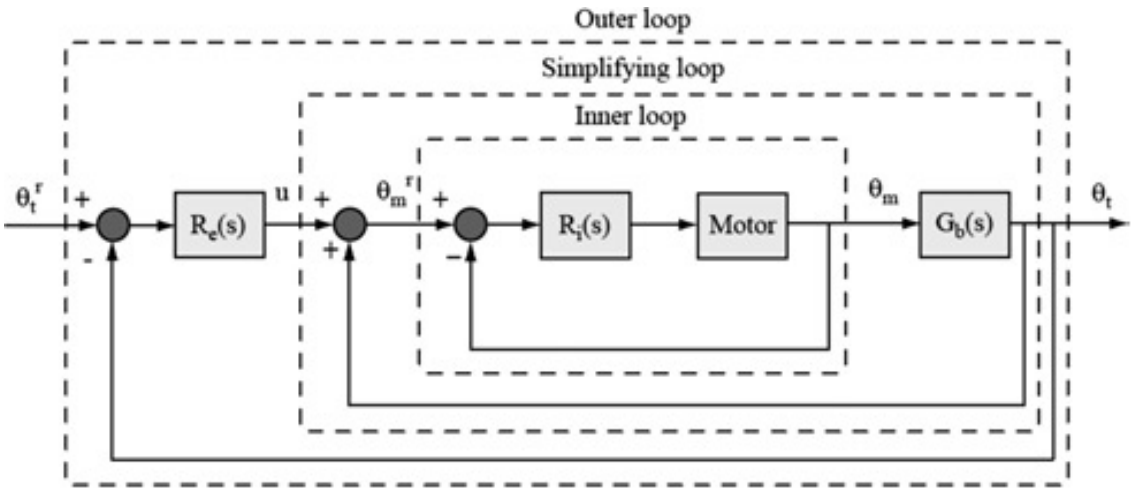


***Figure 2.2.*** *Generalized picture of fractional order controller architecture, featuring three nested loops [36].*

Velocity feedback controller provides effective damping of vibrations and guarantee the stability of the closed-loop system. However, this requires realization of differentiator and it results in a high control effort in all frequencies. Lead Zirconate Titanate (PZT) actuator/sensor systems were very popular among different references. [32, 46]

Repetitive control methods main goal is to track with zero steady state error periodic references and also to reject periodic disturbances. The controller iteratively repeats the trajectory until the effects of the flexibility have been canceled. Only disadvantage is that the method can not adapt into payload changes without modifying point masses. This is because controller can not be applied unless the vibration modes are multiple of the basic frequency. [19, 21]

Fractional order control uses strain gauges to measure the link deflection, which results in more robust controller than other accelerometer measurements. The control strategy, which is shown in figure 2.2, consist of three loops as follows: 1) An inner loop, which controls the actuator and its target is to keep transfer function close to unity. 2) A simplifying loop, which uses positive unity-gain feedback to reduce the dynamics of system. 3) An outer loop, which has the fractional derivative controller, which shapes the loop and gives an overshoot independent of load changes. Drawback of this method is that only linear systems with constant coefficients can be handled. [36]

Singular perturbation control method investigates complex issues by dividing them into different reduced problems and then assembles them together to form a appropriate control. However, solutions for the manifold equations become very complicated and model uncertainties are reflected into slow dynamics of the system. [30, 25, 31]

Generalized proportional integrator control method was used in an experiment, where a flexible robotic arm driven by conventional motor with gear actuator. Angular position of the motor was feedback signal, therefore no other measurements were needed. As disadvantages few things can be mentioned: GPI results in longer response time and period of oscillation than proportional action alone. [8, 7]

Integral resonant control (IRC) aims to change the pole-zero interlacing of a collocated system to zero-pole interlacing. This is achieved by adding a constant feed-though term to the system, which adds a zero at a frequency lower than the first resonant mode [4]. As integral gain is rising, the poles of the system move away from the imaginary axis into the left-half of the complex plane and eventually to the open-loop zero locations. IRC uses collocated sensor/actuator pair to damp active structures. The resonant controllers are modeled such that they approximate the differentiator over a narrow bandwidth, which is around the resonance frequency of the system. IRC is able to damp high resonance vibration and results in precise end point positioning. The structure is also simple and it guarantees closed-loop stability even with dynamics, which are not modeled neither in the range of bandwidth. IRC approach design procedure still requires trial-and-error method to come up with proper feed-through term and integrator gain. Other drawback is that the response does not roll off high frequencies. [38, 32, 4, 37]

Passivity theorem controllers are simple and robust to the changes in arm dynamics, which results in slow motions. Passive approach is also less effective than active version of control. Passive theorem is also prone to the joint friction. Few methods are been proposed, which are resulting more complex controllers. [20, 43, 39]

Adaptive control approaches are also investigated for flexible structures. Sliding-mode has been taken as a example of these control schemes. Other this type of strategies such as robust, neural networks or fuzzy logic, follow similar ideas, and they have common advantages and disadvantages.

Sliding-mode is a nonlinear variable structure control method that modifies the dynamics of system. The modifier is discontinuous control signal, which forces the system to adjust around its normal behavior. Sliding-mode method has been used with fuzzy logic or neural networks. It has the ability to deal with modelling uncertainties, maintain stability, has consistent performance and reduced order of controller. On the down side, it can lead to chatter, energy loss, plant damage and excitation of un-modeled dynamics. [10, 9]

### 2.2.3 Sensor systems

Strain gauge feedback control method utilized strain gauges, which are distributed along the flexible boom. The strain gauges measure the curvature of the beam and the gauges are placed to the positions to catch the lowest frequencies of the bending beam. In [35] the author has placed three strain gauges along the boom to capture the three first modes of the vibration. Gauges were placed at the zeros of the curvature function of fourth mode. The disadvantage of strain gauge measurements is that they don't provide direct information about the manipulator displacement. Instead they demonstrate only local behavior of the beam. Therefore, strain control requires a lot time in order to implement proper control schemes, which are complex and yet still inaccurate. [6, 47]

Acceleration feedback from the boom tip can be used as benchmark for other sensor systems measuring system deflections due to very high vibration detection. It is also used for control, where boom tip position is measured with accelerometer and then fed back to the system. Drawbacks of the acceleration feedback are noisy and often biased signals, which are twice integrated to accumulate the error.[27, 40, 11]

Vision systems are becoming popular position tracking measuring methods, due to growth in computational power. The advantage lies in high reliability compared to the strain gauges. On the other hand, the delay caused by image processing is the biggest problem among the required environment. In literature, there is multiple attempts to overcome the delay, which include Kalman filtering method, extrapolation and other methods. [27, 16, 17]

Other methods to vibration measuring are position sensitive devices, piezoelectric materials, ultrasonic sensors and range sensors. Position sensitive devices have high frequency sensing but they are expensive and they add weight to the boom tip [26]. Piezoelectric materials like lead zirconate titanate (PZT) can be used as a sensor or/and an actuator. They are commonly used in smart structures [14]. Ultrasonic sensor was used in an experiment, where the sensor was placed at the end-effector and the receiver to the hub of the beam. It managed to capture high frequencies and produce accurate position signal. The major disadvantage of this method is highly prone to disturbance caused by surroundings[24]. Range sensors give good and accurate position sensing at high frequencies but it is not very appropriate solution for moving objects, since it has to have fixed reference object. [27]

## 2.3 Discussion

Numerous different kind of control methods were viewed for this chapter, and the amount of control strategies was overwhelming. These ones mentioned were just a tip of an iceberg. Few others to mention which remained outside of this review; state feedback control, bang-bang control, $H\infty$ -control and sliding-surface control.

On the other hand, most of these control methods were tested with a simple flexible link which is driven by an electric servo motor. There were only few applications that were using mobile machines in their studies. Other thing is, that hydraulics as a power source is not very popular among these researches, since the nature of hydro power is nonlinear. Flexible links are also nonlinear, therefore systems with hydraulics and flexible manipulators, result in highly nonlinear system.

***Table 2.1.*** *Comparison of different control schemes.*

| **Control method** | **Measured states/ variables** | **Advantages** | **Disadvantages** | **References** |
|---|---|---|---|---|
| **Feed-forward** | | | | |
| FIR filter | Nominal frequency | Easy | Input delay | [29] |
| Flatness based | None | Accurate | Requires trajectory training<br>Complex | [29] |
| Inverse dynamics | None | Only modal analysis required | May result in inaccurate control | [41] |
| Optimal trajectory planning | None | Efficient path planning | Rely on system compensation | [23] |
| VDC | None | Good vibration damping | Performance depends on operation point | [33] |
| **Feedback** | | | | |
| PPF/NPF | Strain<br>Acceleration | Able to adapt changes | Natural frequency can't vary | [40, 45]<br>[44] |
| Velocity feedback | Strain (PZT) | Closed loop stability | Realization of differentiator<br>High control effort | [32, 46] |
| Repetitive control | Motor angle<br>Torque (strain gauges) | Simple<br>Easy to tune | Vibration modes multiplies of the basic frequency needed | [19, 21] |
| Fractional order | Strain gauge | Varying payloads | Only linear systems with constant coefficients | [36] |
| Singular perturbation | Tip position | Complex issues | Manifold equations become complicated<br>Model uncertainties reflected into slow dynamics | [30, 25]<br>[31] |
| Generalized proportional integrator | Angular position | No other measurements | Longer response time<br>Longer oscillation time | [8, 7] |
| Integral resonant control | Strain<br>Hub angle | Good vibration damping<br>Precise tip positioning<br>Simple structure<br>Closed-loop stability | Trial-and-error method required<br>Response doesn't roll off high frequencies | [38, 32]<br>[4, 37] |
| Passivity theorem controller | Tip velocity | Simple<br>Robust to changes | Slower arm motions<br>Less effective<br>Prone to joint friction | [20, 43]<br>[39] |
| Sliding-mode control | Load position<br>Load velocity<br>Motor velocity | Robust to uncertainties<br>Stability maintaining<br>Consistent performance<br>Reduced order | Chatter<br>Energy loss<br>Plant damage<br>Excitation of un-modelled dynamics | [10, 9] |

# 3. LUMPED PARAMETER METHOD MODELING

Lumped parameter method uses only rigid bodies, joints, springs and dampers in multi-body systems to simulate flexible structures. It is very easy to implement with Matlab Simulink program, when flexible body can be break down to subparts, which have chain like connection. Each subpart may have different geometries. Lumped parameter method approach is sufficient for control design tasks, therefore it is suitable for our needs. [12]

Lumped parameter approach fits to Matlab Simulink modeling environment since it only has rigid body elements. In this method, flexible body in divided into generalized beam elements (GBEs). These parts consist of body-joint-body combination, which then determine the features of the flexible body parts. Implementing lumped parameter method takes the following steps:

1. Break the beam body into separate parts and determine the Degrees of freedom of each element.
2. Use joint in the middle of the each element along the neutral axis (the line through the element that doesn't suffer of streching or compression).
3. Flexible body theory can be used to determine the spring constant for the system, which represents material and geometry features.
4. Add damping to each degrees of freedom.
5. Connect the GBEs to each others with weld joints.
6. Recreate the beam by welding GBEs together.

## 3.1 General beam theory

In lumped parameter method theory, the beam of length $L$ and mass of $M$ is divided into $n$ identical GBEs, where the length and mass of each GBEs are $l = L/n$ and $m = M/n$ respectively. Each joint has damping and spring factors, which are determined by the

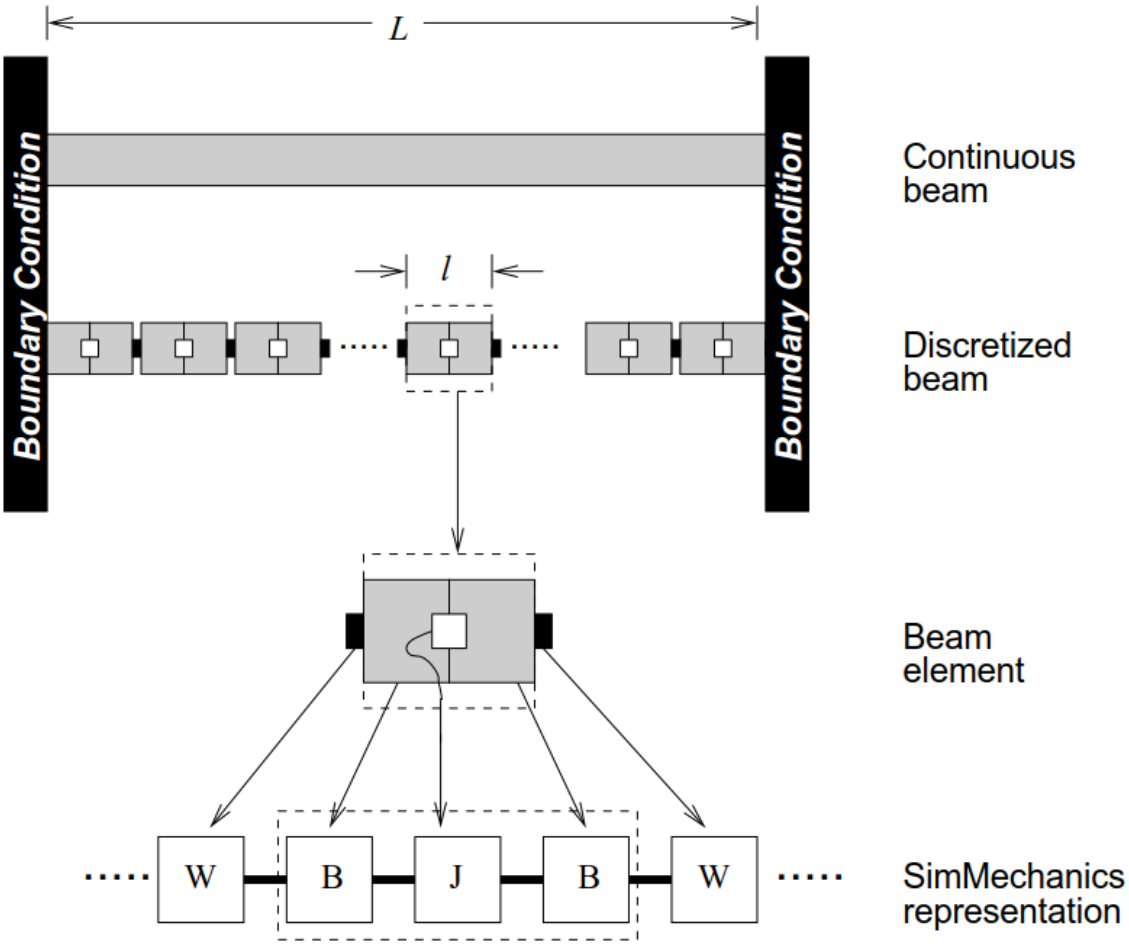


***Figure 3.1.*** *Continuous beam divided into generalized beam elements [12].*

beam properties. General flexibility for the beam is based on assumption, that each GBEs has its own deflection. Figure 3.1 shows how the GBEs are welded together to form a chain of elements, which represents the discretized version of continuous the beam.

One GBE involves two rigid bodies, each length of $l/2$ and mass of $m/2$. Joint is located on the neutral axis of the GBE. For this theory, one end of the GBE is fixed and the other end has $X$ as generalized coordinates and $F$ as generalized forces as shown in the figure 3.2. Let $x$ denote the parameterization of the degrees of freedom of the joint. Now

$$\begin{aligned} X &= g(x) \\ dX &= J(x)dx, \end{aligned} \tag{3.1}$$

where $J(x)$ is the Jacobian

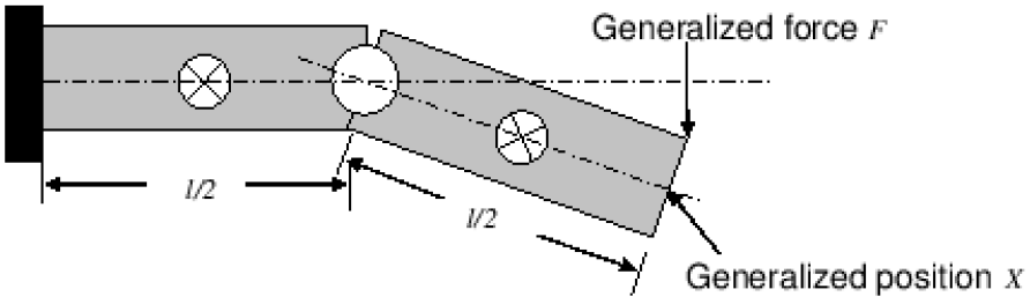


***Figure 3.2.*** *Generalized beam element, which has other end fixed [12].*

$$J = \frac{\partial g}{\partial x}. \tag{3.2}$$

Generalized stiffness matrix $K$ can be used to express the generalized force $F$ at the tip of the GBE:

$$F = KdX. \tag{3.3}$$

Now the generalized force $f$ can be denoted as

$$f = kdx, \tag{3.4}$$

where $k$ is the equivalent spring constant at the joint of GBE and $dx$ is the infinitesimal generalized relative displacement between two bodies across the joint.

The infinitesimal work $F^T dX$ done at the tip of the GBE by the force $F$ is equivalent to the work $f^T dx$ done at the GBE joint by the equivalent force $f$ instead. For any $dx$ can be denoted

$$f^T dx = F^T dX = F^T J(x)dx, \tag{3.5}$$

from which generalized force of the joint $f$ can be driven

$$f = J^T F. \tag{3.6}$$

Substituting equations 3.3 and 3.1 yields

$$f = J^T K J dx, \tag{3.7}$$

so that

$$k = J^T K J. \tag{3.8}$$

Equation 3.7 is the general stiffness expression of a GBE with multiple degrees of freedom.

## 3.2 Beam under pure bending

In this section beam is assumed to undergo only bending without shear. Therefore, beam is modeled having only one primitive revolute joint in each GBEs. This way we have $F = [P, T]$ and $x = [S, \Theta]$, where $P$, $T$, $S$ and $\theta$ are force, moment, vertical deflection and slope respect to the free end of the GBE respectively. Since we have only one revolute joint in this GBE, joint torque is $f = \tau$ and generalized displacement is the joint angle $x = \theta$ as shown in the figure 3.3.

End displacement of GBE $X$ can be formed using linear displacement and rotational displacement

$$X = g(x) = \begin{bmatrix} (l/2)sin\theta \\ \theta \end{bmatrix}, \tag{3.9}$$

and for small values of $\theta$,

$$J \approx \begin{bmatrix} l/2 \\ 1 \end{bmatrix}. \tag{3.10}$$

Now equation 3.8 becomes

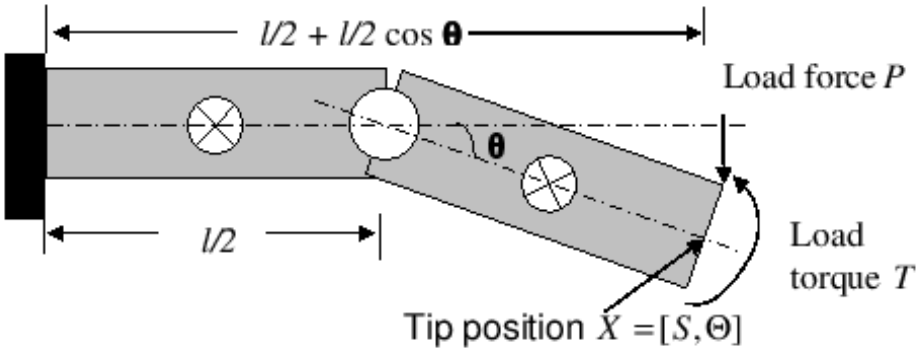


***Figure 3.3.*** *Beam element under pure bending [12].*

$$k = [l/2]K \begin{bmatrix} l/2 \\ 1 \end{bmatrix}. \tag{3.11}$$

Beam theory yields a familiar relation between the deflection, slope, force and moment

$$\begin{bmatrix} dy \\ \theta_\varepsilon \end{bmatrix} = \left( \frac{l}{EI_{zz}} \right) \begin{bmatrix} l^2/3 & l/2 \\ l/2 & 1 \end{bmatrix} \begin{bmatrix} P \\ T \end{bmatrix}$$

or

$$K = \frac{12EI_{zz}}{l^3} \begin{bmatrix} 1 & -l/2 \\ -l/2 & l^2/3 \end{bmatrix}, \tag{3.12}$$

where $E$ is the Young's modulus of the material and $I_{zz} = \int_A y^2 dA$ is the area moment of inertia. This provides us with rotational stiffness or effective torsional spring constant at the joint

$$k = \frac{EI_{zz}}{l}. \tag{3.13}$$

The rotational joint in the $n$th GBE has damped oscillations according to the normalized moment equation

$$\ddot{\theta}_n + 2\xi\omega_0\dot{\theta}_n + \omega_0^2\theta_n = external\ moments,$$

where $\omega_0^2 = k/I$ and $I$ is the moment of inertia. The damping factor $2\xi\omega_0$ is quasi-empirical value that accounts for energy lost to visco-elastic effects. [12]

This formulation suffer from remarkable drawback, since it doesn't correctly represent bending angles. In reality, GBEs aren't independent of each other, thus the bending moment is also dependent on deflection angle of the proximate GBEs. For this reason, discretization cannot be made better by refining. Although this flaw can be fixed by approximating the local curvature and adding this to the local bending moment.

# 4. SIMULATION MODEL

Remarkable part of this thesis is simulation model of the wheel loader, which has been used as real test environment later on. In this chapter the emphasis is on building multi-body model of a four-wheel loader and adding hydraulical functionality, which drives the cylinders of the multi-body model. Modeling of hydraulics has been done in two sections: In the first traditional hydraulical system has been considered, which consists of variable displacement pump, load sensing mechanism and proportional valves. The latter model has variable displacement pump-motor and simple two state valves.

## 4.1 Wheel loader multi-body model

This section deals with multi-body system, which have been used in the simulator. Model has been build with Matlab Simulink Simscape 2nd generation multi-body toolkit. This allows the direct implementation of lumped parameter method, which was discussed in chapter 3. Model is not a complete representation of a wheel loader dynamics. It rather is a very simplified version. Considering the scope of the thesis, boom movement dynamics was the key part of the system. Also wheel deflections were considered worth of taking part of the model. In figure 4.1 the final outcome of the modeling of the multi-body system is presented.

### 4.1.1 Body model

Wheel loader body model consists of wheels and chassis parts. In the wheel section, the ground level is also defined, but it isn't nothing more than a visual surface. World frame is located on a ground level and distance to each wheel is the same.

Front wheels are fixed to the ground from the natural touching point. To add one degree of freedom to the body motions, a revolute joint has been added to ground touching point. This allows the machine to pitch, when heavy load is swinging in front of the machine. During pitching motion, the projection of the rear wheels on the ground layer moves towards the front wheels. Therefore a prismatic joint is needed at rear wheels, which

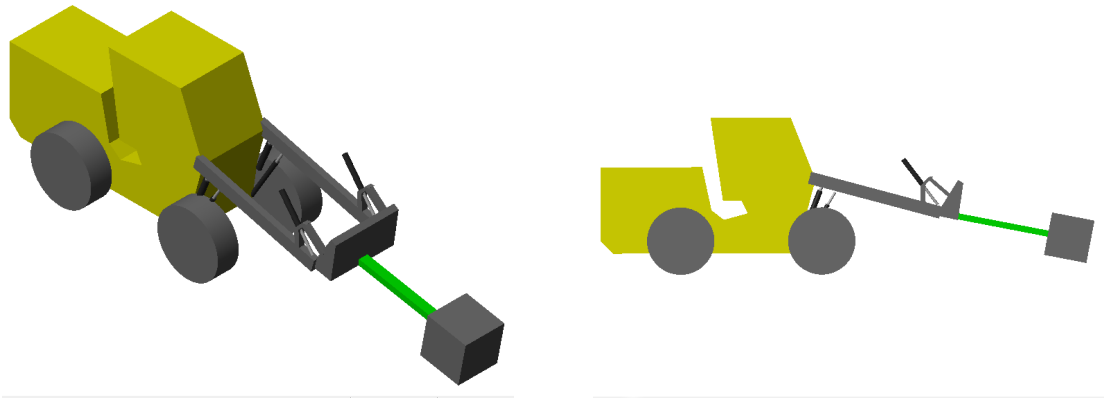

(a) Isometric view. (b) Side view.

***Figure 4.1.*** *Whole multi-body model, where green boom section represents the flexible part.*

allows them to slide along the ground surface. Rear and front wheels define the locations of the rear and front axes, which are used to connect chassis to the wheel model. To simulate wheel deflection when under pressure, each wheel has prismatic joint with spring and damping constant. These parameters are shown in the table 4.1.

***Table 4.1.*** *Wheel model parameters.*

| **Wheelbase (m)** | **Track width (m)** | **Wheel radius (m)** | **Wheel width (m)** | **Spring factor ($\frac{N}{m}$)** | **Damping factor ($\frac{N}{m/s}$)** | **Wheel mass (kg)** |
|---|---|---|---|---|---|---|
| 2.286 | 1.510 | 0.546 | 0.375 | $1.5 \cdot 10^6$ | $3 \cdot 10^4$ | 100 |

During the simulations, the machine is meant to stay in its place, thus there is no need to model anything that is related to driving the machine forward or backward. Despite this model allows machine to only pitch. Other rotational angles are not allowed. Pitching has one boundary condition: each wheel has to touch the ground all the time. During the simulations this doesn't cause problems, thus additional modeling isn't necessary.

Chassis model defines the rear and front bodies of the wheel loader. It also defines few other frames, which are utilized in boom model discussed in detail in section 4.1.2.

***Table 4.2.*** *Body model parameters.*

| | **Front body (kg)** | **Rear body (kg)** |
|---|---|---|
| Mass | 1617 | 2436 |

Body model physical dimensions are not exact, since no detailed information was available for accurate modeling. Only rear and front masses of the bodies were at hand, which

are 2436 kg and 1617 kg respectively. Since the goal wasn't to produce accurate model of the wheel loader, instead rather a good approximation of mobile machine dynamics when operating with boom, which is prone to vibrations.

### 4.1.2 Boom model

Boom model is the most important part of the multi-body model, since it has every single one of the hydraulical actuators the model has. It also represents the flexible boom part, which is shown in the figure 4.2 using green color.

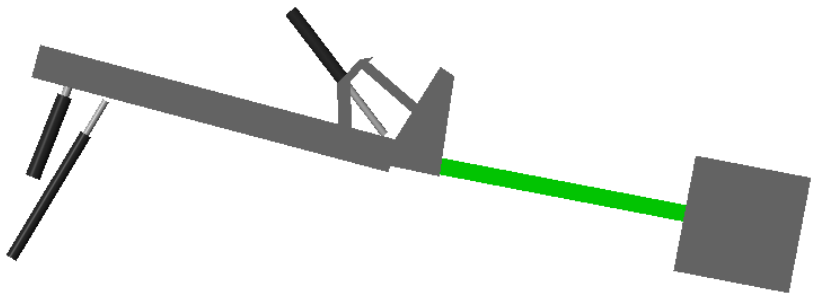

***Figure 4.2.*** *Boom model presented with multi-body toolkit from side view. Part highlighted with green, represents the flexible section of the boom.*

Physical parts of the boom, such as main beam and attachment frame, include many inaccurate values such as mass and dimensions. Only known parameters were the joint locations, which were used to approximate the physical dimensions and masses of different parts. These minor inaccuracies do not chance the simulation outcome drastically. Boom model parameters have been listed in table 4.3, where $x$ and $y$ plane forms the cross-section of the boom. Dimension $z$ defines the depth of a part.

Boom has three different sets of cylinders, which are lift, tilt and stabilizer cylinders, where one set consists of two cylinders. These are discussed more in section 4.2, but from multi-body modeling view there is few points worth mentioning. Cylinders have primitive prismatic joint, which defines movement direction of piston. Hydraulics model

calculates the force, which is fed to the cylinder model. This force defines the velocity of the piston respect to the dynamics of the whole multi-body model.

Boom dynamics can be simply modeled by using revolute joints, and joint positions are defined by using rigid frame transformations. Each joint frame have been calculated respect to the joint, where boom attaches to front chassis.

***Table 4.3.*** *Boom model parameters.*

| | Dimensions (mm) | | | Mass |
|---|---|---|---|---|
| | **x** | **y** | **z** | **(kg)** |
| **Rigid boom** | 2200 | 200 | 100 | 250.0 |
| **Attachment** | 350 | 680 | 1135 | 300.0 |
| **Bar** | 285 | 370 | 100 | 20.0 |
| **Link beam** | 60 | 457 | 100 | 2.7 |
| **Flexible boom** | 1500 | 100 | 150 | 50.0 |

Boom consists of left and right sides, which are then connected together with an attachment frame, which is used to attach auxiliary equipments, such as pallet fork or bucket. In this case, flexible boom is attached as an auxiliary equipment. At the end of the flexible boom lies a load, which mass will be changing in order to simulate different type of scenarios. Load is defined as a point mass, but it is visualized as rectangular box for the sake of clarity.

Flexible boom section follows the lumped parameter method, which was discussed in chapter 3. Boom is divided into 10 equal GBEs, and assumed to undergo pure bending. Joint between the rigid body parts is primitive revolute, and it has spring constant and damping factor values of 320 990 $\frac{Nm}{deg}$ and 283.28 $\frac{Nm}{deg/s}$ respectively. These factors haven't been validated by any means. They are chosen with iterative method and simulation, which showed they provide enough features to simulate bending boom.

## 4.2 Hydraulics model

Hydraulics model simulates a system, which has traditional proportional valves combined with variable displacement pump system controlled by load sensing functions. Hydraulics model calculates cylinder forces, which are then fed to the multi-body model. Hydraulics section can be divided into subsections of supply system, valves, hoses and cylinders. These component models are discussed in this section. Since the real machine has variable displacement pump-motor and digital valves, this model has been modified in order to replicate the features of digihydraulic system. These modifications are discussed in this section.

Like already mentioned in section 4.1.2, boom has two parallel lift, tilt and stabilizer cylinders. Lift cylinder function is to raise the whole boom, and tilt cylinder tilts the attachment frame. Stabilizer cylinders add fluid flow into tilt cylinders, when boom is being lowered and vice versa. As a result, attachment frame stays leveled, even though the boom height is changed using lift.

Variable displacement pump flow calculated in a following method

$$Q = \eta_{vol} n V_k, \tag{4.1}$$

where $\eta_{vol}$ is pump volumetric efficiency, $n$ rotational speed of the pump and $V_k$ is pump displacement per revolution. In pump model, $V_k$ is variable and its value depends of the actuator pressures and pump input pressure. $V_k$ includes also swash plate and pressure compensator valve dynamics. Pump generates flow, which is fed into supply line model, which yields

$$\Delta p = \frac{(Q - \Delta V)B}{V}, \tag{4.2}$$

where $V$ is volume system, $Q$ flow into the system, $\Delta V$ the change in the volume, and $B$ the bulk modulus. For this case, the volume is assumed to be constant.

Valve simulation model includes load sensing (LS) functionality and proportional valve openings. LS procedure selects the highest pressure at the actuators, which is then used as a reference pressure at the pump model. Proportional valve model includes basic equations, which give valve spool some dynamical features. Bi-directional flow equations with cavitation choking are used to determine the flow though the valves. Each flow path is calculated separately.

The hose model is the following one after the valves. First this model determines the pressure inside the hoses and then transforms it back to flow using same formulas as the valve flow path model. Pressure can be derived from the equation 4.2, which determines the pressure inside a volume, which was previously used in the pump model. The volume of the hoses is assumed to remain constant.

Cylinder model uses the same equations as mentioned before. Force $F$ produced by the single cylinder chamber can be calculated using $F = pA$, where $p$ is the pressure in the cylinder chamber and $A$ is the effective area of the piston. In order to get the total force of the cylinder, the counteracting forces have to be taken into account. These are the force of the B side of the cylinder and friction force.

Chamber pressure can produced by equation 4.2, but in this case chamber volume is non-constant. Volume inside the chamber can be calculated as

$$V = Ax + V_h + V_0, \tag{4.3}$$

where $A$ is the area of the piston, $x$ the piston position, $V_h$ the volume of the hose and $V_0$ the dead volume of the cylinder. Since the volume is changing as a function of x, bulk modulus $B$ also varies as a function of $V$

$$B(V) = \frac{VB_oB_h}{VB_h + V_hB_o}, \tag{4.4}$$

where $B_o$ and $B_h$ are the bulk moduli of the oil and hoses respectively.

Cylinder models use combined Stribeck and tanh friction model to calculate friction force $F_f$ caused by the piston, which is sliding along the lubricated surface. According to [3] the model can be formulated as

$$F_f = (F_c + (F_s - F_c)e^{-(|v|/v_s)^i})\texttt{tanh}(k_{tanh}v) + k_v v, \tag{4.5}$$

where $F_c$ is Coulomb sliding force, $F_s$ maximal static friction force, $i$ an exponent, $k_{tanh}$ model tuning parameter, $k_v$ viscous friction coefficient, $v$ sliding speed and $v_s$ sliding speed coefficient. Sliding speed is determined by the velocity of the piston. These parameters are listed in the table 4.4.

***Table 4.4.*** *Parameters used in the combined Stribeck and tanh friction model with different cylinders.*

| **Cylinder** | $F_s$ (N) | $F_c$ (N) | $k_v$ (N/(m/s)) | $v_s$ (m/s) | $k_{tanh}$ () | $i$ () |
|---|---|---|---|---|---|---|
| Lift | 1500 | 1000 | 1500 | 0.015 | 4000 | 2 |
| Tilt | 1500 | 1000 | 1500 | 0.030 | 4000 | 2 |
| Stabilizer | 1500 | 1000 | 1500 | 0.030 | 4000 | 2 |

Cylinder models don't include end modeling, besides a simple stop simulation block. Cylinder end model isn't important, since the goal is to drive cylinder models within the range.

# 5. EATON CMA MOBILE VALVE

One commercial application, which uses load damping, is Eaton CMA mobile valve, which is shown in figure 5.1. It is a mobile valve, which uses sectional block layout and enabled by CAN bus to provide wide range of services for the user. Eaton offers two different size valve assemblies, one with 90 and the other with 200 flow rate. In this section, the Eaton CMA200 mobile valve has been inspected in detail. [1]

***Figure 5.1.*** *Eaton CMA mobile valve block. [1]*

Eaton CMA mobile valve layout consists of inlet and working sections, the latter providing flow to the actuators. Inlet section provides port for supply pressure, tank and depending on customer selection a load sensing port for LS system can be chosen. Since customer has an option to combine multiple valve block assemblies together to form greater

systems, a extension inlet can be installed to the block. Only one inlet pressure controller is required in the system. [1]

The working section consists of two independent spools as seen in figure 5.2. These can be paired to work as a regular spool to control actuators, which required double acting services. Due to independent controls of the spools, one block may control two single acting actuators. Each mainstage 3-position 3-way directional spool is controlled by 3-position 4-way pilot spools.

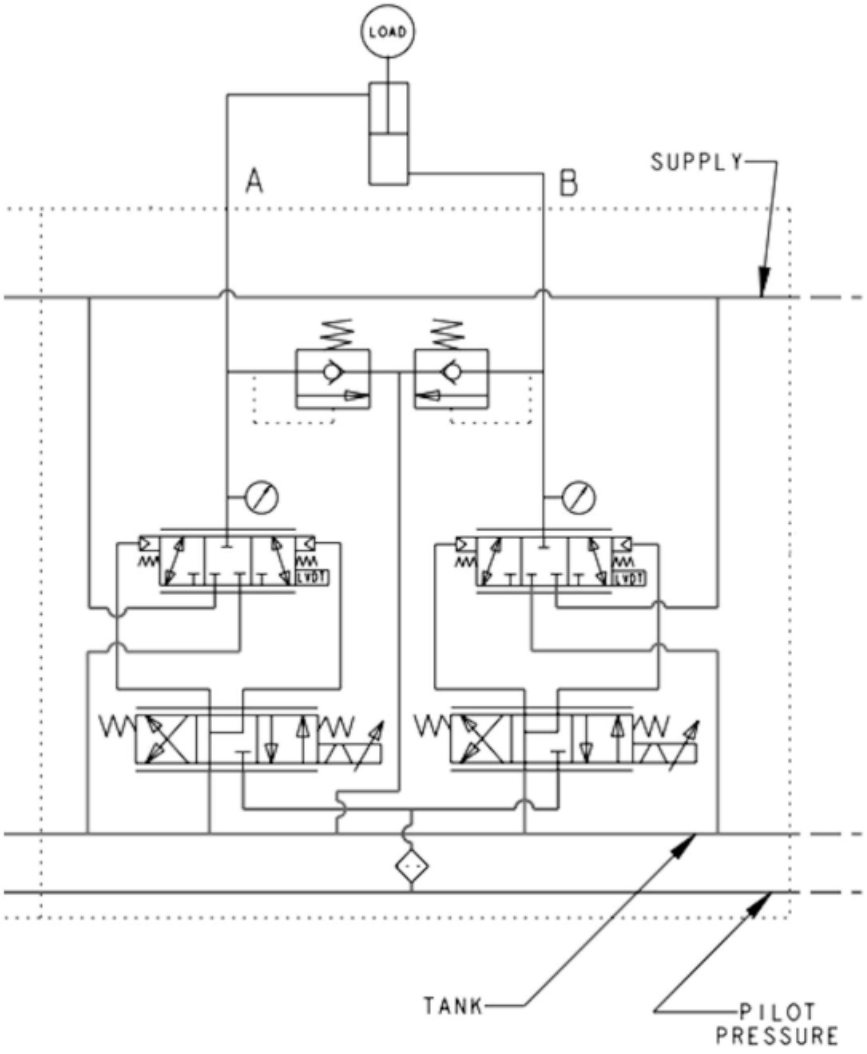


***Figure 5.2.*** *Single working section block of the CMA mobile valve. Modified from reference [1].*

Pilot spools are controlled by on-board micro controllers, and control algorithms are used locally with aid of sensors located around the valve assembly. Each mainstage spool position is measured, which allows spool position control. Moreover, each port has integrated pressure sensor, which allows flow control. [1]

Valve block communicates with CAN bus, which utilizes CANopen or J1939 protocols upon customers choosing. When valve block is connected to the CAN bus, it is seen as one node and it operates on 250 kb/s with J1939. CANopen can be configured to use 125, 250 or 500 kb/s. Moreover, identifiers of 29 and 11 bits are used when operating with J1939 and CANopen, respectively. [1]

Valve block controller features various software based control methods, which include pressure and flow compensated controls for single and double acting actuators. In addition, several other special case control features can be utilized, that are electronic load sensing, load damping, flow sharing (with capability to prioritize) and spool position control. Software also allows diagnostics of sensor data. Few other software based services and control packages are available, that are torque control, hose burst detection and limp mode, which allows system to continue operations at limited level, when sensor malfunctions. [1]

# 6. CONTROL SCHEME

This chapter deals with different control methods, which have been used during this thesis. The main focus will be at pressure feedback and damping of structural vibration. Since the real test machine utilizes variable displacement pump-motor, digital valves and control code, which is running the system, thus pump control code is carefully examined. This pump code is also tested in simulation environment.

## 6.1 Control of proportional valve system

In this section load pressure as feedback signal is discussed. The idea behind this method is that instead of measuring bending with strain gages or accelerometers, pressure in the cylinder chambers could be used to estimate the vibrations of the boom.

### 6.1.1 Pressure feedback controller

In the simulation case where boom movements are controlled with proportional valves, a simple negative feedback loop is used to damp boom vibrations. This control method is built on a valve spool controlled open loop system. Command reference is given via a joystick, which opens the valves accordingly.

For the controlling purposes load pressure is defined

$$P_L = \frac{2(p_A - \lambda p_B)}{1+\lambda}, \tag{6.1}$$

where $p_A$ and $p_B$ are cylinder chamber pressures and piston area ratio $\lambda$ is defined as $A_b/A_a$, where $A_a$ and $A_b$ are cylinder piston areas. Load pressure yields zero when cylinder force output is zero.

Cylinder is usually holding up a load, which means $P_L$ being non-zero. Therefore a filter is required to counter any effects of a load. In this case, a transfer function is utilized with following form

$$TF(s) = \frac{\tau s}{\tau s + 1}, \tag{6.2}$$

where $\tau$ is constant value of 0.17.

Reference signal is directly used to control the valve spool position when controller is driven with open loop manner. In closed loop simulation the control law is

$$y(u) = u - k_{P_L} P_L \tag{6.3}$$

where $u$ is reference signal and $k_{PL}$ is pressure feedback gain.

### 6.1.2 Feedforward command shaping

During the very first test, it became clear, that pressure feedback didn't suppress the vibrations completely, especially when the first swings of the load occurred. Therefore a command shaping filter was added to the controlled, which was meant to smooth the command signal when transitions from state to another happened.

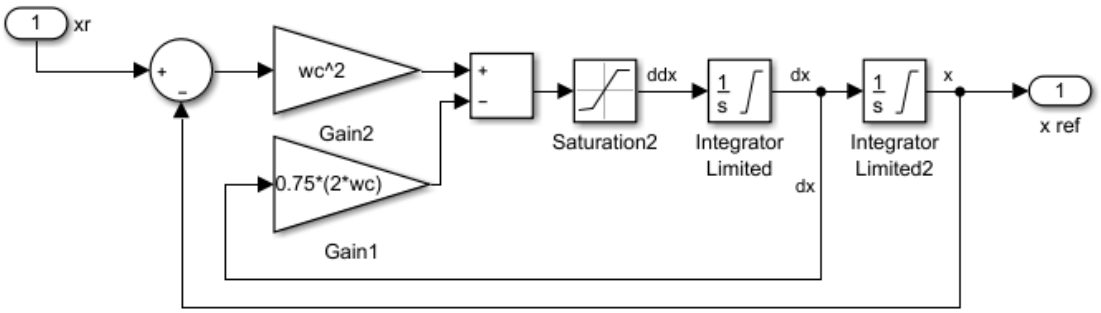


***Figure 6.1.*** *Command shaping filter, which uses input reference signal $x_r$, limits acceleration, velocity and position to yield $x_{ref}$.*

For command shaping, a reference generator in figure 6.1 was used. Filter yields $x_{ref}$, which satisfies acceleration, velocity and position limits as well as bandwidth $\omega_c$.

For this controller the position limits are the same as valve spool, which are from -1 to 1. Bandwidth $\omega_c$ can be chosen depending on the dominant resonance. The smaller $\omega_c$ results in better vibration damping but at the cost of higher command lag. In this case 10 rad/s has been used, which should give good command response as well as vibration damping.

## 6.2 Control of digital valve system

Digital valve and variable displacement pump-motor system is being controlled with pump controller, which operates the valves and pump-motor swashplate angle. This is the core of the control scheme, which has been modified for the vibration damping purposes. These modifications are discussed in separate subsection.

### 6.2.1 Pump controller

Pump controller code has two parallel controllers, and both of them have their own functions. One is displacement controller, which controls the boom movements, and the other is pressure controller, which controls the pressure at the supply line. A simple block switches between these two controllers, where as valve opening decides the control mode. These two parallel controllers are discussed in this section.

### 6.2.2 Displacement control

Displacement controller moves the boom respect to the joystick command. Controller working principle is shown in figure 6.2 and functions as follows. Joystick signal is scaled into desired velocity, which is then transformed into pump displacement. This transformed reference is then used as a pump control current. Pump output flow is measured, scaled to pump displacement and used as a feedback signal for the controller.

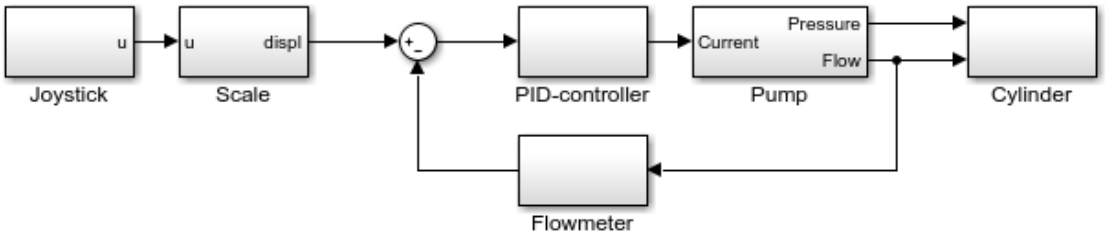


***Figure 6.2.*** *Simplified visualization of displacement controller.*

Variable displacement pump is able to work as a motor as well, which allows negative swashplate angles, therefore it is possible to transform work done by gravity back to the engine.

Variable displacement pump determines the speed of actuator, and valves define the direction of motion as in figure 6.3. In valve controlling section, the core decision making

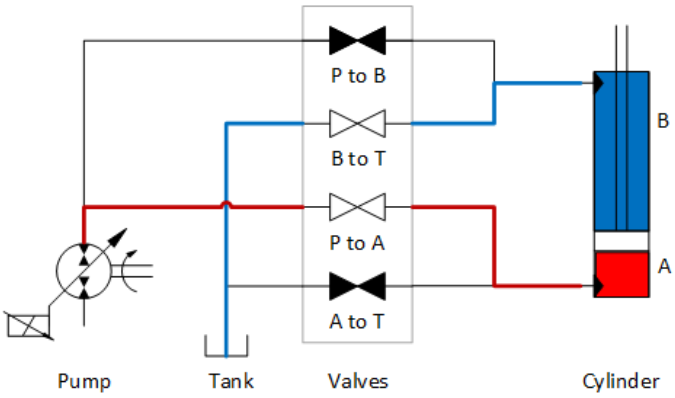


(a) Lifting and lowering mode.

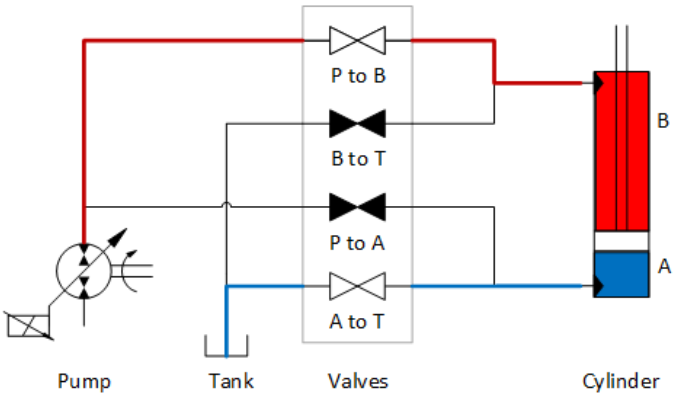


(b) Pressing mode.

***Figure 6.3.*** *Flow paths when a) pump is lifting or lowering the load and b) when so called pressing mode is initiated. Pressing mode can be also used when load mass isn't enough to bring the load down.*

signal is given by joystick. This decides the desired motion direction. When lifting the load, flow paths from pump (P) to cylinder A chamber and from B chamber to tank (T) are opened. In load lowering motion, there is two options: Option one (1) is to use the pump to force load down by opening P to B and A to T. The other way (2) is to use pump as a motor and let the gravity push the load down. In this case flow paths P to A and B to T are opened. Pressure in the actuator A chamber is measured and used to determine, which lowering method is utilized. When pressure is low, which means bucket or auxiliary device is on the ground or the weight of the load doesn't give enough velocity during the lowering motion, therefore option 1 is used. When actuator A chamber pressure is above the threshold, option 2 is used to lower the load. It is also possible to use different type of flow paths, which allow fast motions such as differential connection, but they are not used during this experiment.

To prevent major hydraulical impulses in the system, valves are not opened and closed

instantly then the movement command is given. Valve controller doesn't allow flow paths to be opened until the pressure difference over the valve is less than a threshold value of 10 bar. When joystick is returned to the zero position, controller waits for 0.1 s before closing the valves. This value is different for tilt and lift actuators.

Valve controller also prevents flow paths to tilt and lift cylinders from opening at the same time. This also means, it is not possible to operate tilt and lift motions simultaneously. Diesel engine being off also prevents any operation of valves.

### 6.2.3 Pressure control

The other controller, which is required for pump controlling functions is pressure controller. Since displacement controller acts mainly when operator requests movement via joystick, pressure controller focuses on the actions when valves are closed.

The main task of pressure controller is to keep supply pressure at 30 bar constantly. This is the case when joystick is at zero position. When operation requests movement, pressure controller increases or decreases the supply pressure, depending on the cylinder force direction, until the pressure difference over valve is satisfied.

Pressure control requires pressure measurements from multiple locations. These are pressures at supply line and in every cylinder chamber. Since measuring pressure is difficult task due to noise, a filter is required. During this experiment a Geometric Moving Average (GMA) filter [42] is being used to suppress unwanted noise, which is defined

$$y(k) = (1 - \alpha_{gma})y(k-1) + \alpha_{gma}u(k), \tag{6.4}$$

where $\alpha_{gma}$ is a filter parameter and $u$ is the signal to be filtered. For this case the value of 0.04 has been used for the $\alpha_{gma}$.

### 6.2.4 Vibration damping control

Vibration damping control is not really a separate controller, since it is better described as extension to the displacement controller. This means, that vibration damping adds few features to the valve and displacement control sections.

For the displacement part, controller is pretty much the same as it for the proportional valve controller, which was discussed in section 6.1. Pressures at the cylinder chamber are

measured and load pressure $P_L$ is calculated with equation 6.1. To eliminate drift caused by load, $P_L$ is filtered using transfer function presented in equation 6.2 and multiplied with factor $k_{vib}$. As a result the displacement controller yields a control signal $Q_{cmd}$

$$Q_{cmd} = Q_{ref} - k_{vib}P_L - Q_{meas}, \tag{6.5}$$

where $Q_{ref}$ is desired displacement and $Q_{meas}$ measured pump displacement. PID-controller is used to yield control signal for the pump. The whole combined controller is shown in figure 6.4.

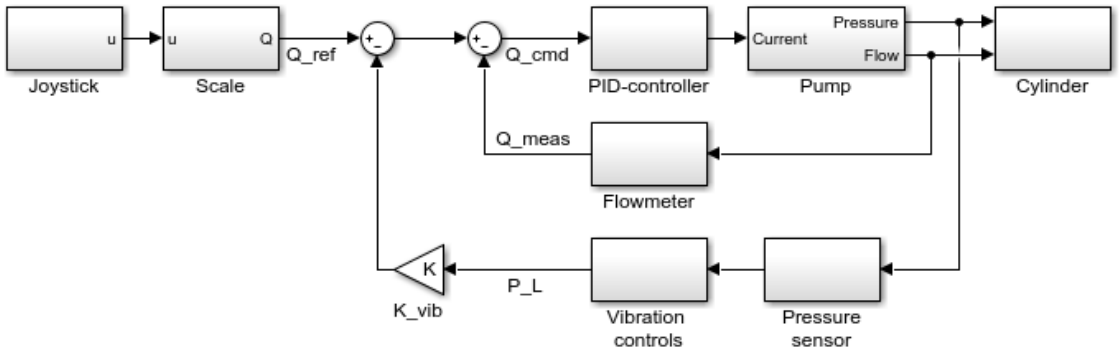


***Figure 6.4.*** *Simplified visualization of displacement controller, where vibration control has been added.*

As mentioned in section 6.2.2, when joystick is returned to the zero position and displacement controller keeps the valves open for 0.1 s. This may cause remarkable oscillations in the system (structural and hydraulical). Thus another controller is added for the valves, which extends the period before the valves are closed. This also gives displacement controller time to react oscillations properly.

Vibration detection module has been added to the system, which has two purposes: it can force the system switch between pressure and displacement control modes, and open the valves. Vibration detection uses same method to estimate the boom oscillations as the other controllers, which have the load pressure feedback. Load pressure is used to determine, whether the boom is vibrating or not. If load pressure value rises above the threshold, controller forces the displacement control. Vibration detection stays triggered until the load pressure hasn't rose above the threshold during the last 0.3 seconds.

# 7. REAL TIME TEST ENVIRONMENT

For real machine implementation, Wille front wheel loader has been used, called as IHA-machine. This machine, pictured in figure 7.1, has been modeled in chapter 4, and in this chapter the real machine assembly is discussed.


***Figure 7.1.*** *IHA-machine wheel loader with extended crane mounted to the tilt frame.*

IHA-machine has a length of 6.5 m, width of 2.0 m, height of 2.8 m. It weights total 4000 kg and it has front and rear chassis [5]. Steering is applied with articulated-frame-steering system. Different types of auxiliary equipments can be mounted to the boom, but in this case pallet fork with extended crane has been used in order to create flexible and long boom. A load weight of 100 kg has been attached to the tip of the boom.

## 7.1 Work hydraulics

IHA-machine work hydraulics has been implemented with parallel cylinders in tilt and lifting motions. In addition, stabilizing cylinders working as passive actuator keeping the

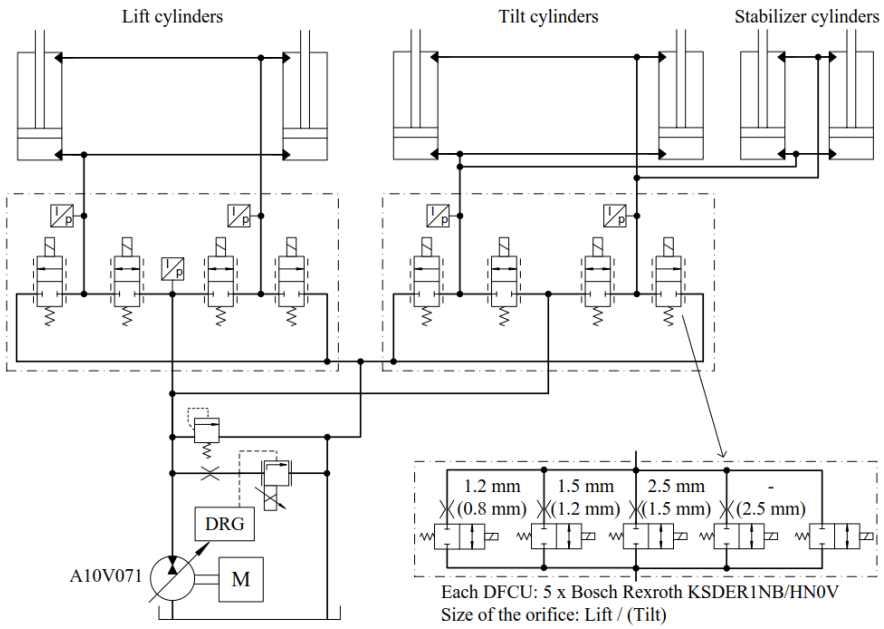


***Figure 7.2.*** *IHA-machine work hydraulics represented [5].*

mounted equipment leveled when boom is lifted or lowered. These motions are each controlled by four digital flow control units (DFCU), which each having 5 parallel connected on/off-valves as shown in figure 7.2. DFCU valve blocks have port pressure sensors, which are needed for pump and vibration control. Work hydraulics also have pressure relief valve as a safety measure to prevent supply pressure reaching dangerous levels. [5]

Hydraulic work circuit has a variable displacement pump-motor as power source. It has electrical load sensing function called DRG, which sets the pressure limit. It also can be remotely controlled with external pressure relief valve, which in this case can be set with pump control code. [22]

## 7.2 dSPACE

The main controlling unit for working hydraulics is dSPACE Microautobox pictured in figure 7.3. It is used to collect sensor data, control the boom movements via CAN bus and run the pump control code. dSPACE allows easy implementation of Matlab Simulink using RTI block set, therefore models generated with Simulink can be complied and downloaded to the Microautobox.

Control Desk 5.4 has been used as graphical interface during real time experiments. It allows changing the code variables while model is being executed, and monitoring as well as recording any signals that Simulink model has. Control Desk runs on a laptop and


***Figure 7.3.*** *Microautobox used to control the boom and collect data from the sensors [15].*

it is connected to Microautobox via Ethernet.

## 7.3 Communications

The entire control system has been build on CAN buses (except flow meter), which are using CANopen or J1939 protocol. The system consists of multiple buses as shown in the figure 7.4. CAN1 acts as main bus, enabling high level communications of the system. CAN1 also enables IHA-machine to use autonomous or teleoperation control, but these are not utilized during this thesis. [5]

CAN2 and CAN3 are sub-buses, where actuators and sensors are connected to. Microautobox controls separate digital hydraulics bus, which transmits the lift and tilt valve commands and receives the sensor data from port pressures. CANmeas bus is used to connect the IMU to the communications system. [5]

## 7.4 Flow measuring

Flow in the supply line is measured by the gear type flow meter manufactured by Kracht. Movement of the gears in the housing are sampled with two sensors, which generate two channel output for better resolution in addition to flow direction recognition. [28]

Flow meter is connected directly into dSPACE using DIO encoder input, which calculates the gear rotation speed as impulses per second. Using the knowledge of sensor resolution,

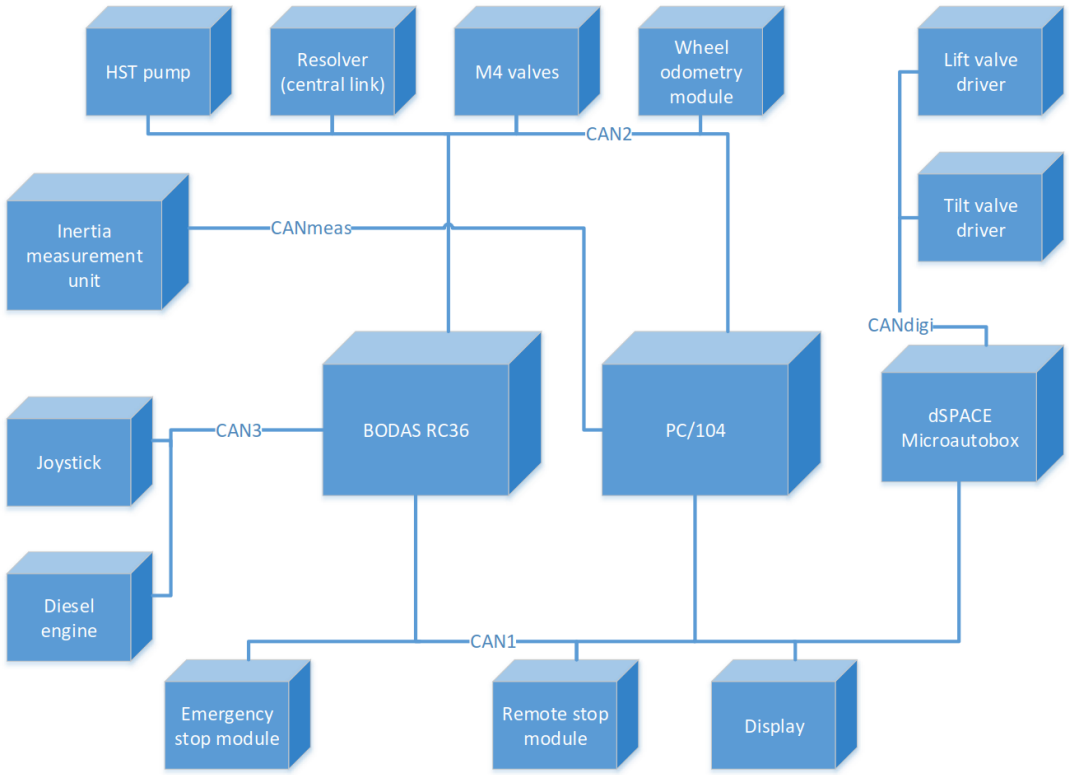


***Figure 7.4.*** *The CAN communications system layout.*

the flow can be calculated. Flow meter is connected directly to the IHA-machine batteries, which give 24 V voltage and circuit is protected by 3 ampere fuse.

## 7.5 Executable model

In order to build a executable model to Microautobox, the pump code had to be discrete time. During the simulation a continuous time transfer function has been used, which had to be discretized. This was done using Matlab *c2d* command, which transforms the continuous transfer function into discrete version.

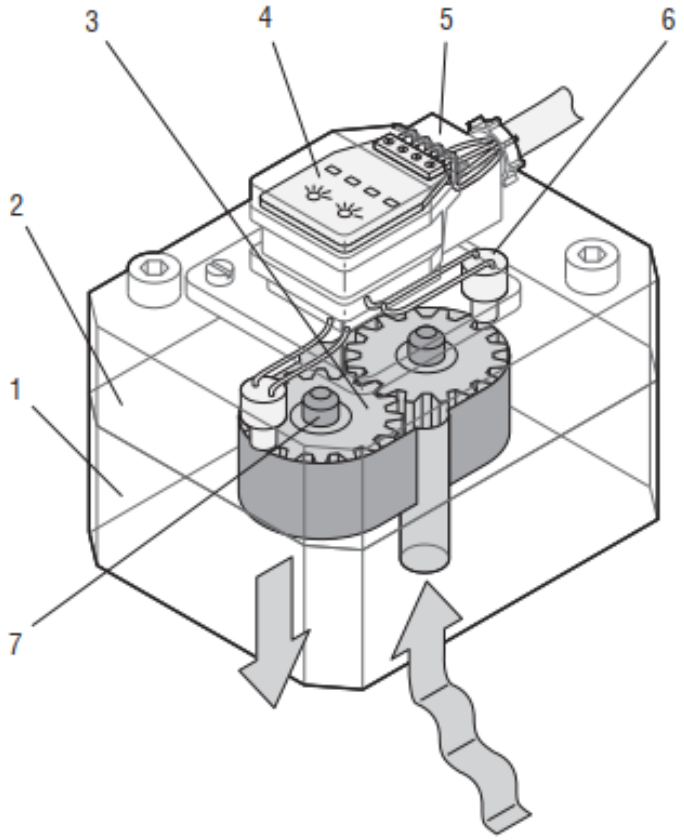


***Figure 7.5.*** *Kracht gear type flow meter. 1) Housing 2) Cover 3) Gear 4) Preamplifier 5) Connector 6) Sensor 7) Bearing assembly [28]*

# 8. RESULTS

In this chapter the simulation and real machine test results are represented and discussed. Figures are generated using Matlab in both simulation and real machine cases. This chapter structure is following: First the simulation results of proportional valve system are discussed, followed by digital valve system. At last real machine results are discussed.

## 8.1 Simulation

This section of simulation results has been divided into two subsections: proportional valve and digital valve controlled sections. The wheel loader simulator remains the same, meanwhile valves and supply unit varies.

Simulation model is capable of producing multiple sources of vibrations. First one is boom structural oscillations are measured using azimuth angle, which represents the difference between the mounting frame and boom tip. Second source is fluid compression, which can be seen as cylinder piston vibrations. The third one is tire deflection, which have been noted as difference compared to the ground level. This means, when the tire radius is greater than the distance between tire axle and ground level, tire deflection shows negative digits.

### 8.1.1 Proportional valve control

Proportional valve simulations are carried out so, that the open and closed loop control methods could be compared easily. Also multiple different scenarios were used to simulate various cases, where damping using load pressure could become handy. These cases were:

Lifting tilt
Lowering tilt
External force
External impulse

Also iterative method have been used in search of optimal parameters for controller gains, which includes variation in start angle of the boom and load mass.

(a) Boom at starting position. (b) Boom at end position.

***Figure 8.1.*** *IHA-machine simulation boom positions during the positive tilt motion.*

During the lifting tilt motion, which is shown in the figure 8.1, the reference for the valve has been given as the figure 8.2 shows. Valve accepts control commands from range of -1 to 1 and the control loop sample time is 20 ms. Command signal seen in the figure has been chosen due to various reasons. In the beginning two second long settling has been added, since the initial parameters of the simulator are not accurate. The step magnitude of 0.2 and duration of the open time is optimized to allowing system vibrations settle during motion but still reaching the fastest possible velocity and remaining in the reasonable boom operation range. The simulation time is long enough for the system to settle after the valve has been returned to the zero position.

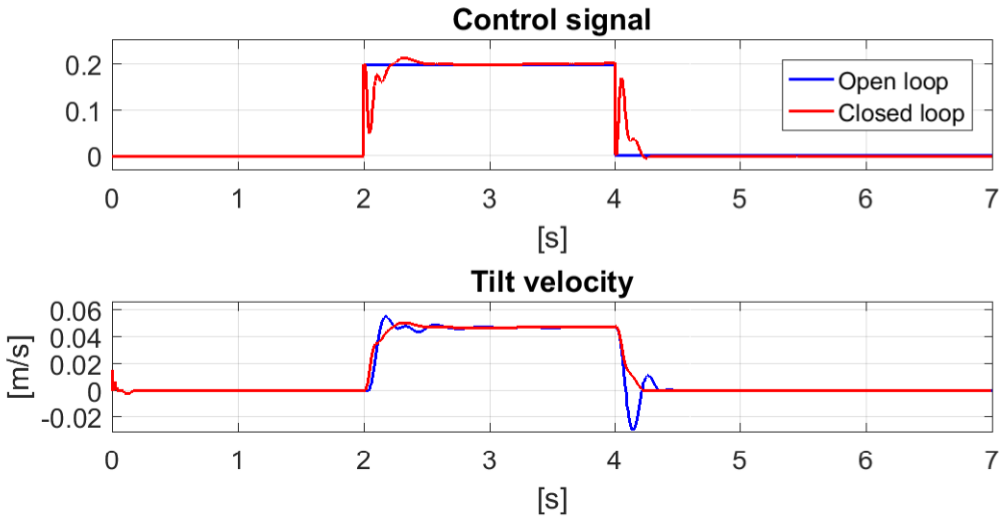


***Figure 8.2.*** *System behavior when tilt is raised for two seconds at constant rate.*

Red line shows the vibration damped and blue line represents the open loop system in figure 8.2. After the motion begins, the feedback system first decreases the acceleration and then increases it, to match the load pressure differences. Tilt cylinder velocity reveals the vibration caused by fluid compression, which are clearly present during open loop

simulation and are significantly reduced when the feedback loop of the tilt cylinder load pressure has been added.

Successful system damping can also be seen in figure 8.3, where boom bending is described using azimuth angle. Feedback system appears to be working as intended countering boom bounces, especially at the stop of the boom motion, where the amplitude of oscillations is larger.

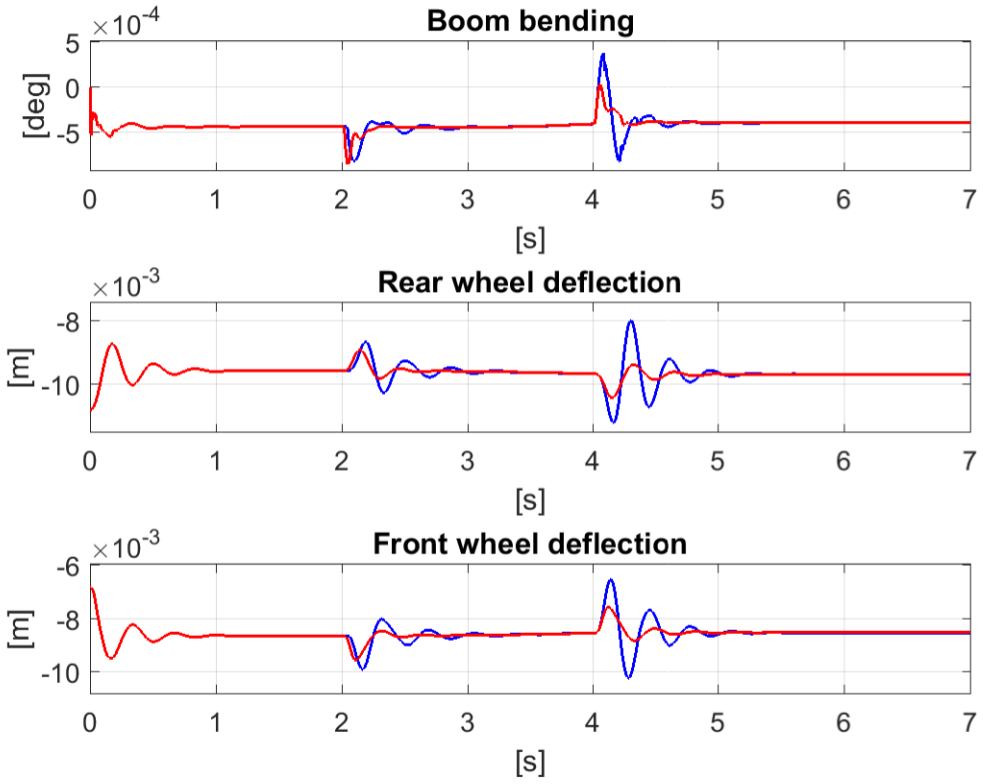


***Figure 8.3.*** *System behavior when tilt is raised for two seconds at constant rate.*

Wheels are usually a common source of vibrations, which holds true in this case. Therefore pneumatic compression at the wheels was also measured to see if the vibrations were suppressed. As we see in the 2 bottom pictures of the figure 8.3 the oscillations have been damped similar way as they were in boom bending figure. This also confirms the assumption, that oscillations from multiple sources can be damped by controlling the boom movements.

Finding optimal pressure feedback gain was also tested with iterative method using the simulator. This would have led into feedback gain as a function of tilt angle. Pressure feedback gain was tested with multiple different values, masses and several set points, which were chosen around the feasible boom operation range. Simulations showed that changing the initial position of the boom or payload mass didn't effect on feedback gain

performance. Therefore the system was decided to be driven with a gain, which had the best performance.

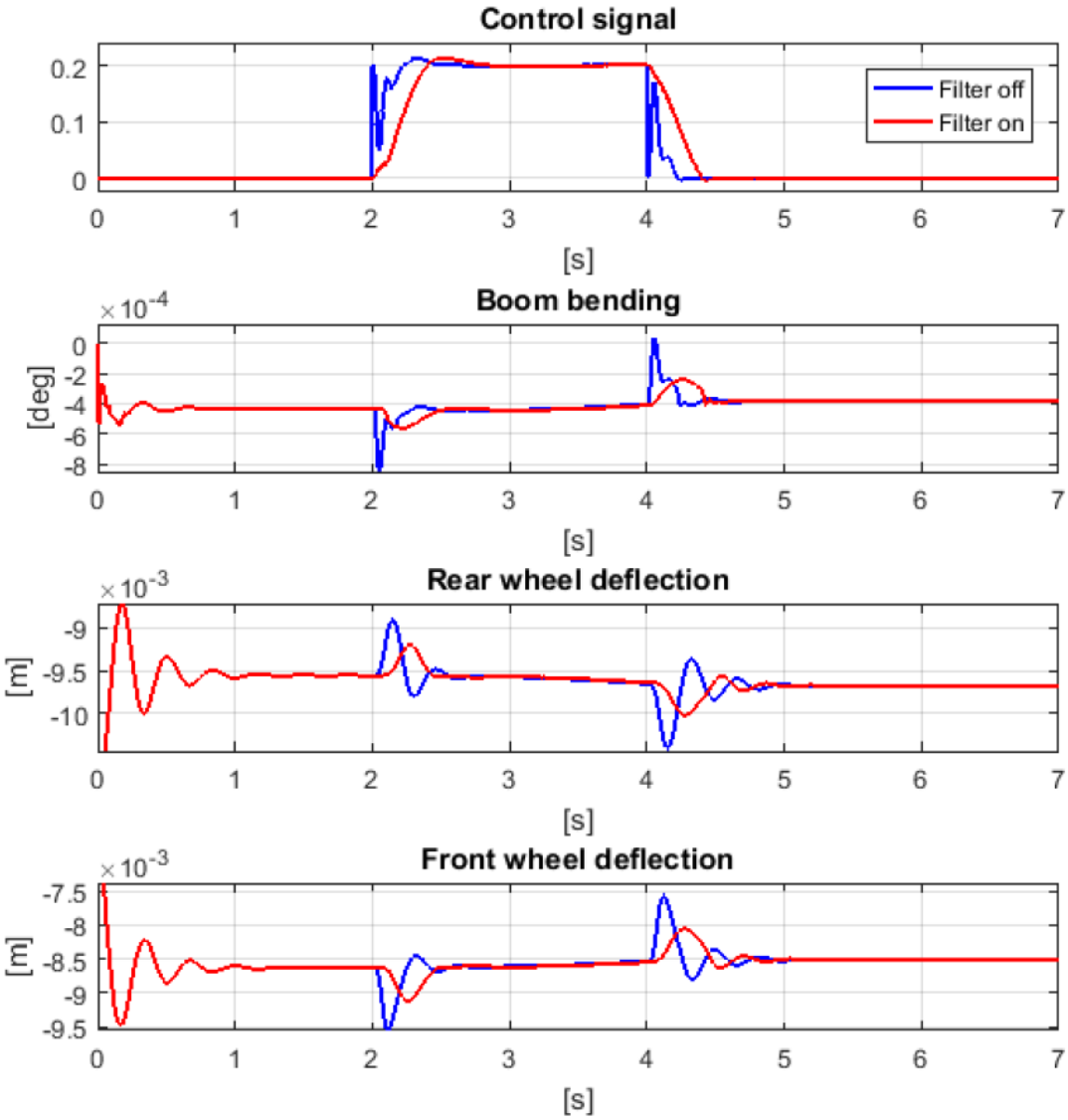


***Figure 8.4.*** *System behavior when using pressure feedback with and without command shaping.*

Test results discussed previously showed promising vibration damping after the first swing has occurred. This couldn't be damped with pure pressure feedback control, because the nature of feedback system: they can't predict the future. Therefore a command filter was implemented, which smooths the input reference as seen in the figure 8.4.

System vibrations are damped in command shaping case by the cost of step response speed. The biggest advantage of this method is the initial swing being suppressed efficiently. Despite this, the duration of oscillations remains roughly the same. Moreover,

command shaping does work only in situations when operator is giving movement commands. Cases, where vibration is caused by external factor, such as sudden change in load mass, or external force is affecting to the boom, command shaping method does nothing.

For external force tests, simulator with same initial values have been used, and simulation time of 7 seconds has been chosen. At 2 second mark, external mass of 100 kg has been added to the tip of the boom, doubling the existing mass.

In figure 8.5 boom bending and wheel deflections have been pictured. Boom vibrations are smoother with closed loop control, but oscillations at wheels are suppressed efficiently. This means that the machine operator should feel a lot less distractions when operating controlling devices.

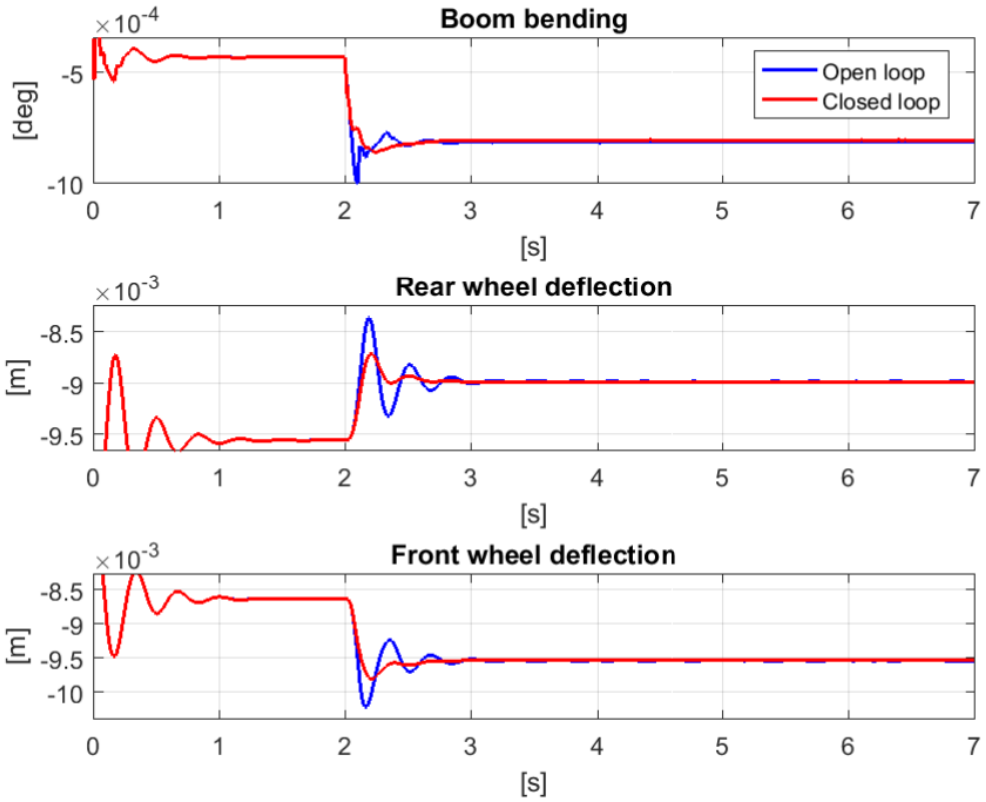


***Figure 8.5.*** *Feedback system performance when excited with external mass of 100 kg.*

When system was tested with motion, which lowered the load, the results were very similar compared to the lifting motion. In order to avoid repeating the previous discussion, these results are bypassed due to similarity. Furthermore external force and impulse test ended up having very similar results, thus are not discussed separately.

### 8.1.2 Digital valves with pump control

In this section, simulator with variable displacement pump-motor has been used. Flow to the actuators is controlled by on/off valves, and each flow path is controlled by single valve, resulting four valves for tilt cylinder. Other reason for these simulations is testing the pump control code, which is used with real test machine also. Simulation should give good guide lines for IHA-machine behavior.

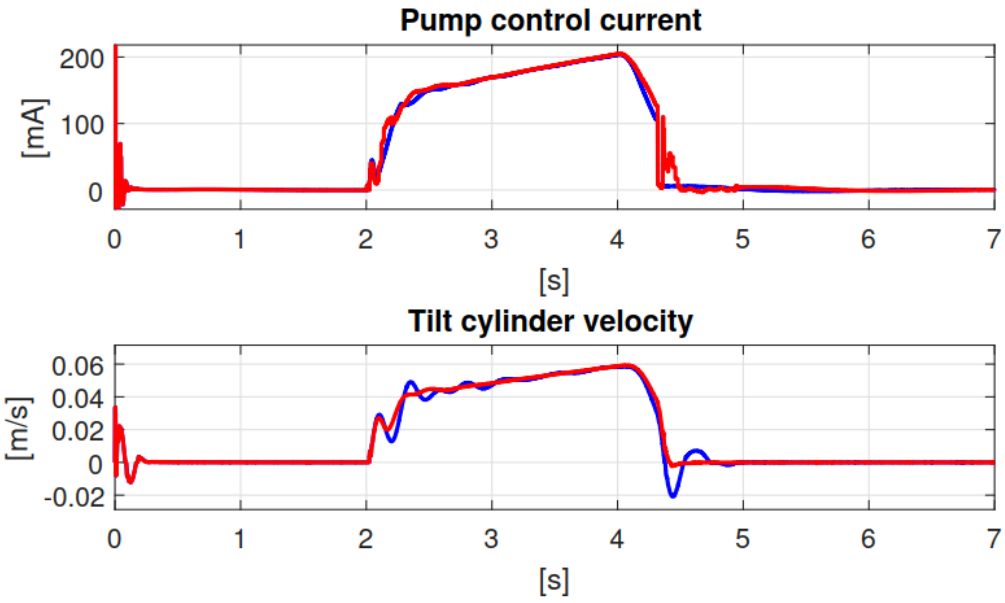


***Figure 8.6.*** *Pump control signal and boom tilt cylinder velocity.*

Simulations are driven with similar method as in proportional valve case, where open loop refers to the case, where vibration damping feedback is not used. This doesn't mean all feedback signal are disabled, since pump supply pressure and flow are significant feedback values for pump controller functions.

In figure 8.6 system behavior has been pictured, when load is lifted. Lifting command starts at 2 second mark, lasts for 2 seconds and ends when the simulation has been running for 4 seconds. Figures compare the system performance when operated with and without pressure damping function, which are drawn with red and blue lines respectively.

Proposed vibration damping method seems to be efficient in pump control case, as the vibrations occurred during the open loop simulation situation have been suppressed in a satisfactory manner as shown in figure 8.7. This holds true to both motion starting and stopping events. As noticed in section 8.1.1, after the initial swing, the system damps the following oscillations. This can be seen in both boom and wheel graphs.

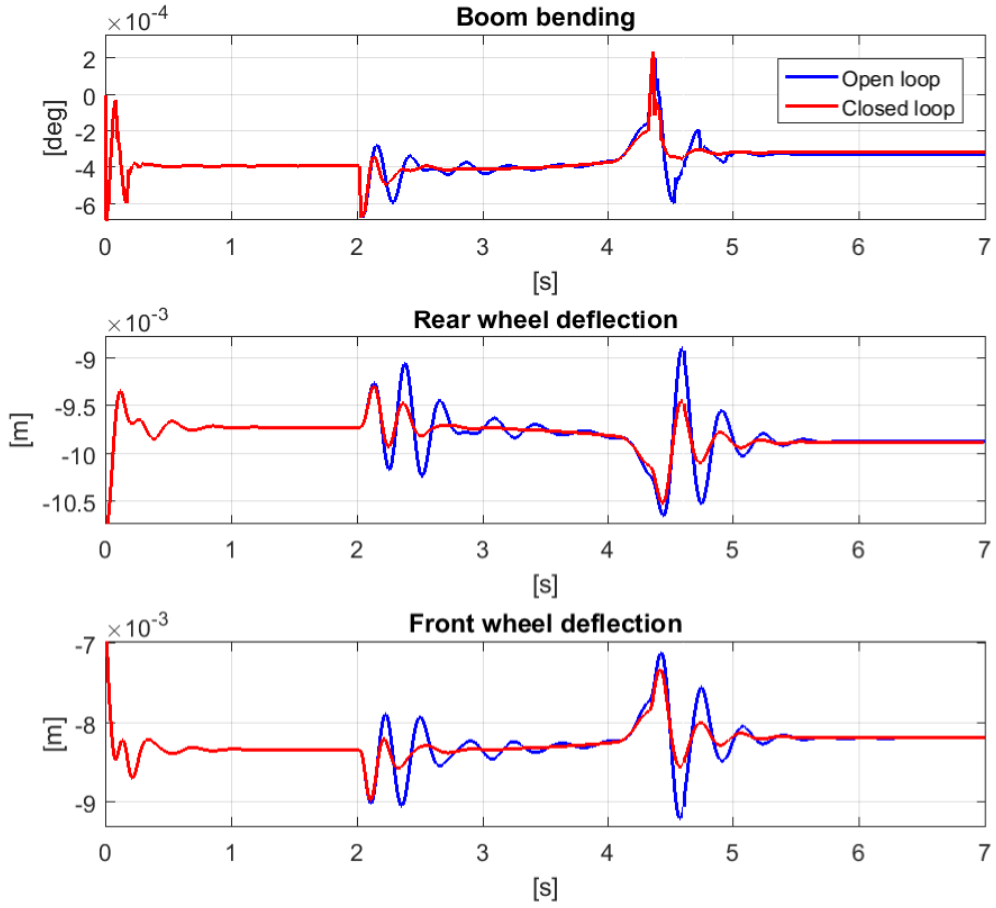


***Figure 8.7.*** *Boom bending and wheel deflections during open and closed loop pump control.*

Due to improvements in load stabilization during and after the motion, the pressure in the system and in the cylinder chambers can be contained as seen in the figure 8.8. This also clarifies the behavior of the pressure control of the pump code, which goal is to keep the system pressure at 30 bar, when valves are closed. During the open loop simulation, the B chamber pressure goes to zero after the valves are closed. This causes possible air bubbles, which may reduce the lifetime of the system due to cavitation.

The valve behavior is visualized in figure 8.9, where flow path from P to A and from B to T is shown. The other flow paths remain closed during this simulation. The control mode is switched at the same moment as the valves shift from state to another. When pressure in the cylinder chambers was a lot higher than 30 bar, the valves were not opened until some time has passed. Reason to this lies in pump control behavior, where system pressure is adjusted so it matches the cylinder chamber pressure before the valves are opened. The same sort of delay can be seen, when motion stop command is given at the time when 4

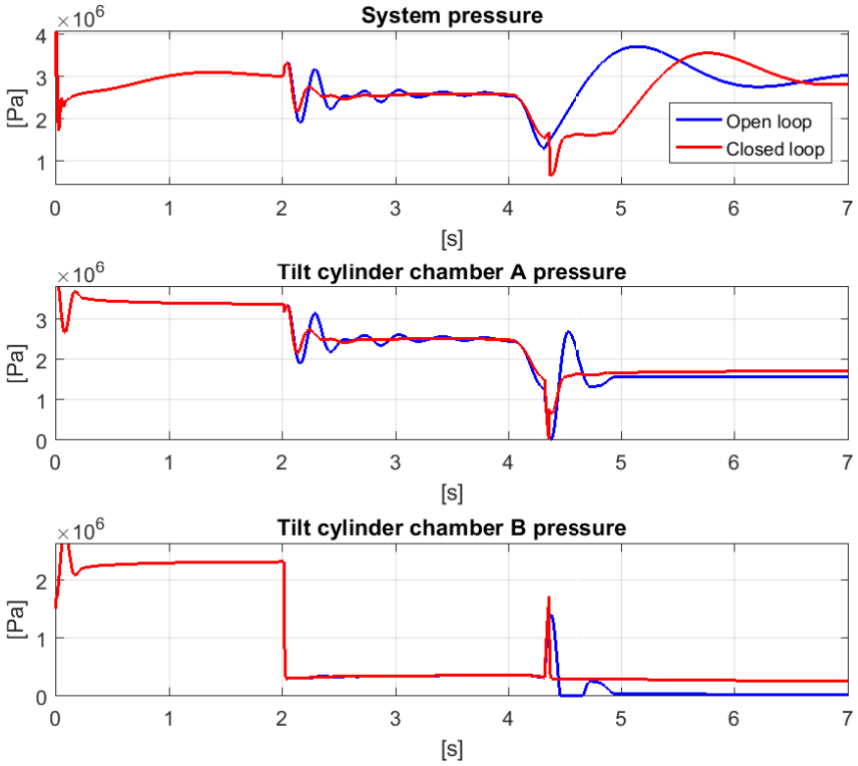


***Figure 8.8.*** *Supply pressure and tilt cylinder chamber pressure in open loop and vibration damping modes.*

seconds has been passed, the valves remain open and pump starts to decelerate. This lasts for 0.3 seconds and it prevents the valves from being closed when cylinder is moving at substantial speed.

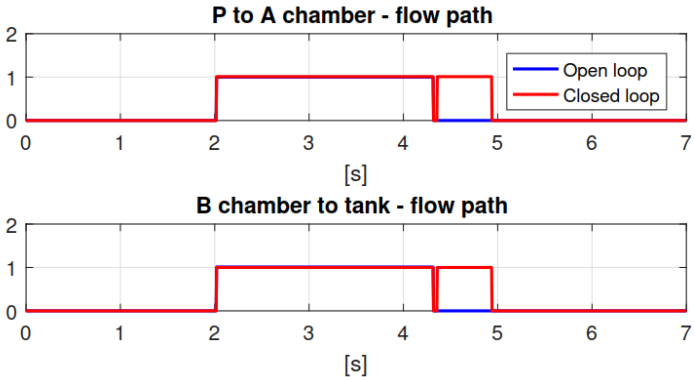


***Figure 8.9.*** *Flow paths from supply pressure to A chamber of tilt cylinder and from B chamber to tank.*

One flaw can be seen in the figure 8.9, when joystick in returned to the zero state, and

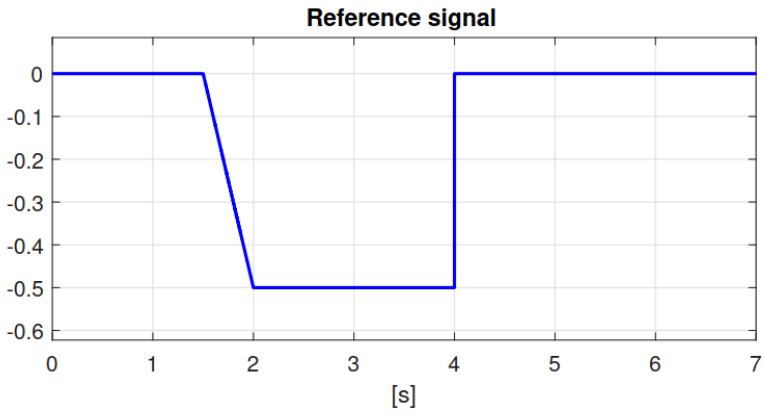


***Figure 8.10.*** *Reference tilt signal for lowering the load.*

valves are close but opened at the next moment. This happens because at the stopping moment, the vibration detection hasn't noticed a deflection big enough, which would trigger the vibration damping sequence. Therefore valves are closed, which causes the sudden spike in the load pressure. This event then triggers the vibration damping sequence. In some other cases this might not even happen, since the deceleration of the boom causes enough deflection in the vibration detection module and damping is triggered pre-emptively.

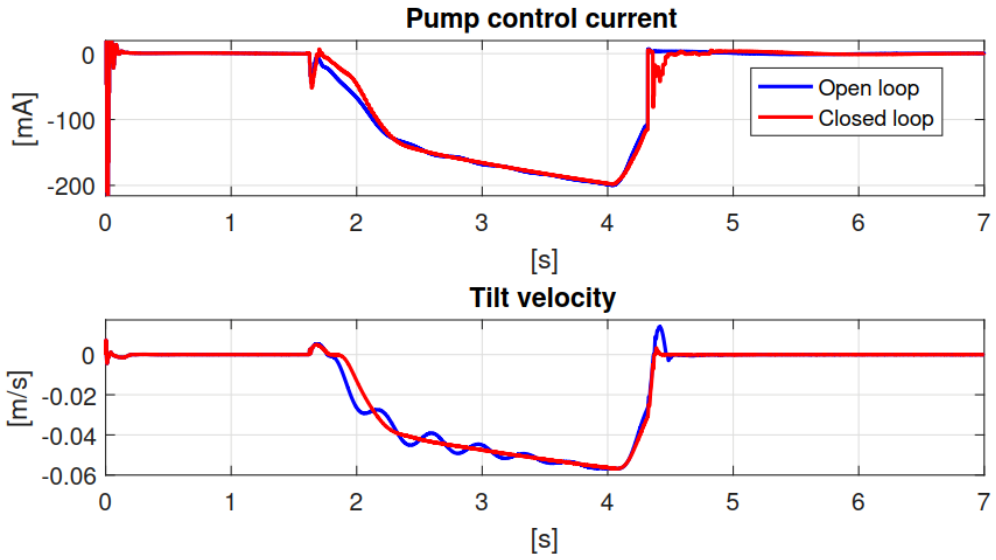


***Figure 8.11.*** *Pump control current and tilt velocity during open and closed loop controls when lowering the load.*

In case of load lowering, a slightly different reference signal has been used. In figure 8.10 a ramp can be seen, which has been added to the beginning of the signal. Without the ramp, A chamber pressure drops to zero, which causes pump controller change to pressing

mode. This is meant for cases, where bucket is already on the ground and operator wants to press the bucket against the surface.

In figure 8.11 the pump control current and tilt velocity is shown. In the open loop section, the tilt velocity seems to drift a lot compared to vibration damping method. Since the pump control figure doesn't show any visible counteractions for vibration, the pressure feedback gives only a small movement commands compared to the major flow control.

The tilt velocity in figure 8.11 also means vibrations in boom, which is confirmed in figure 8.12. Strong vibrations are also present at wheels, which are also suppressed, when the boom isn't oscillating during the motion. When the system stops, there is only a little vibration damping.

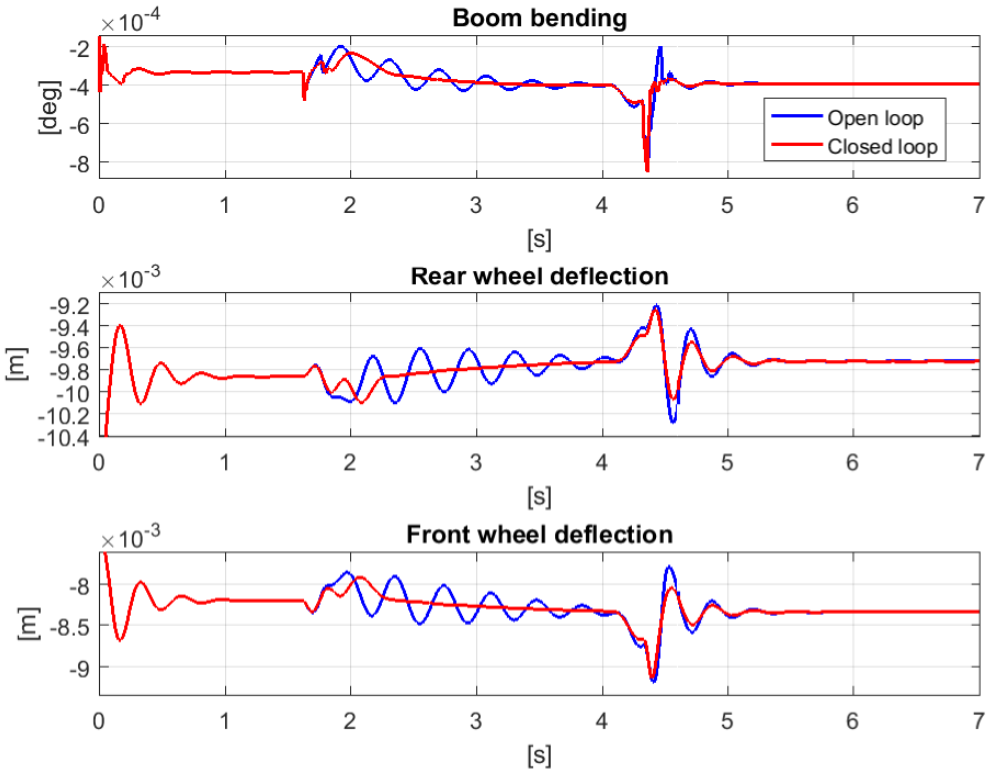


***Figure 8.12.*** *Boom bending and wheel deflections during open loop and vibration damping modes.*

In figure 8.13 it is shown, why vibration damping lower only the amplitude of the oscillations. Tilt chamber pressures are not vibrating at all during the open loop control when the movement stops. Therefore pressure feedback doesn't see any vibrations in the system and does nothing.

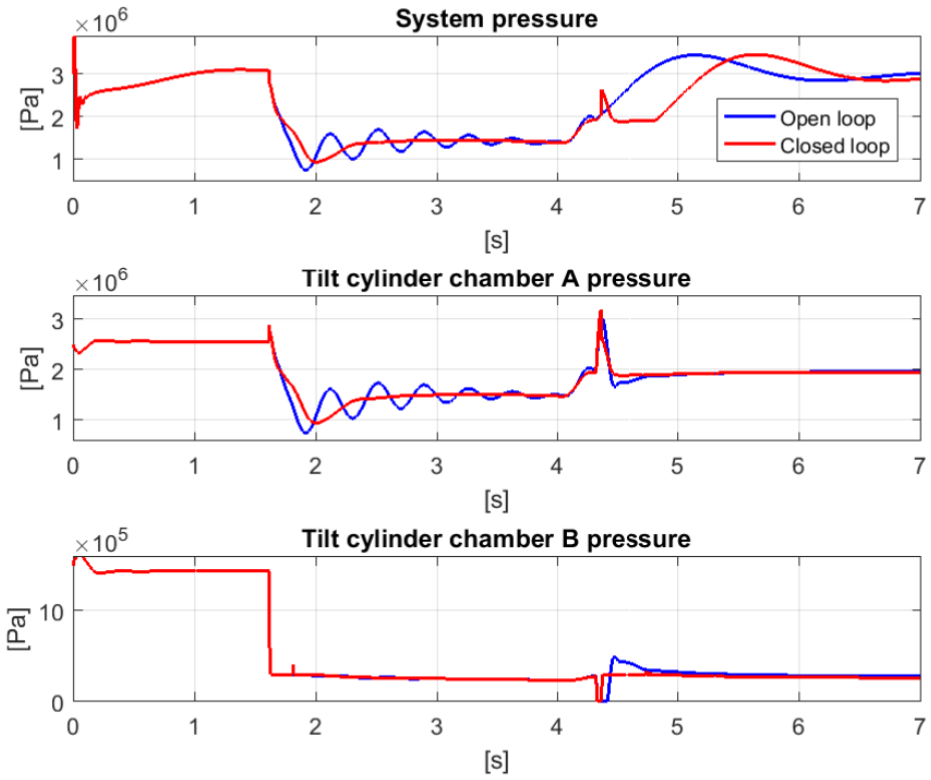


***Figure 8.13.*** *Supply pressure and tilt cylinder chamber pressures during open loop and vibration damping modes.*

Valve openings figure 8.14 shows, that vibration damping is triggered after the motion has stopped. This was obvious, since cylinder chamber pressure are spiking at that moment.

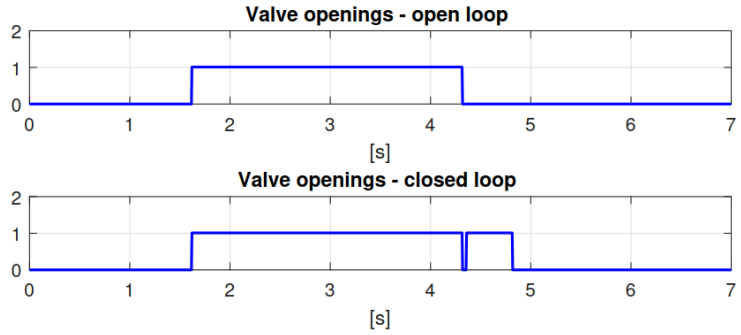


***Figure 8.14.*** *Flow from supply to tilt A chamber and from B chamber to tank. Upper figure in open loop and lower in vibration damping case.*

When simulating system with bigger load, the results remained pretty much the same. One notable difference was that the amplitude of vibrations grew larger, which was expected. External force simulations showed very similar results as in proportional valve section, therefore repeating these results is not necessary.

Simulations show potential, which lies in the vibration damping with load pressure. It suppresses oscillations all around the machine, which were modeled and observed. Few drawback was also found, such as lowering the load utilizing gravity. It seems to be dependent of load mass, since naturally more weight provides more force downwards.

## 8.2 Real test environment

In this section the test performed with real machine are shown and discussed. During this thesis, the lifting and lowering motions are done using the tilt cylinder only, which was the main focus when designing the feedback controller. During the test phase, a inertial measurement unit (IMU) was added to the end of the boom to meter acceleration in order to estimate the performance of the feedback system.

Tests were performed on a flat ground, since any surface angle results very different vibrations in the wheels. Moreover, the way how the load was attached to the tip of the boom is shown in figure 8.15, caused vibrations also in horizontal direction.

***Figure 8.15.*** *Load attached to the tip of the boom. Arrow indicates the added swinging direction due to fastening method.*

In the test phase, the operator uses the joystick to move the boom to the desired direction. Lift cylinder services are not used during the test runs, even though the combination of lifting and then damping with tilt could be another interesting topic. Due to nature of human operations, every single work sequence (lifting when lowering) is unique. Therefore an exact comparison between these two in not possible. Instead, some general conclusions can be drawn from the test runs, which are discussed.

### 8.2.1 Lifting the load

In the following figures open loop and vibration damping mode test runs are plotted on top of each other. This makes it easier to compare and evaluate the performance of feedback system. In figure 8.16 joystick reference and tilt cylinder position are shown. As mentioned before, a human operator can not produce two identical inputs to the system, but should be enough to make some conclusion regardless.

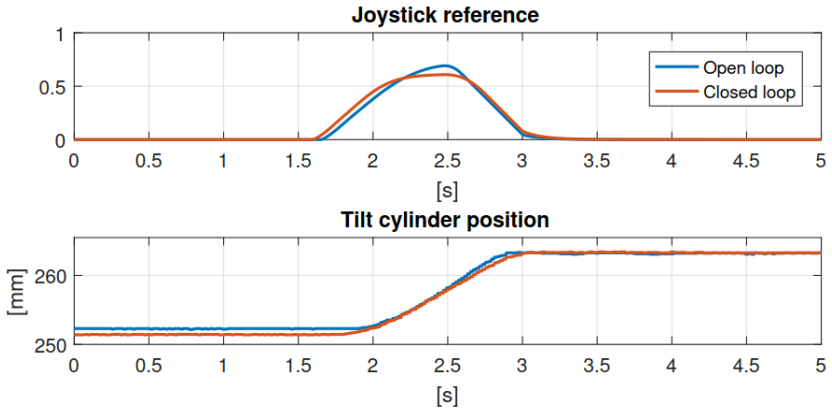


***Figure 8.16.*** *Real machine control command given by joystick and tilt position.*

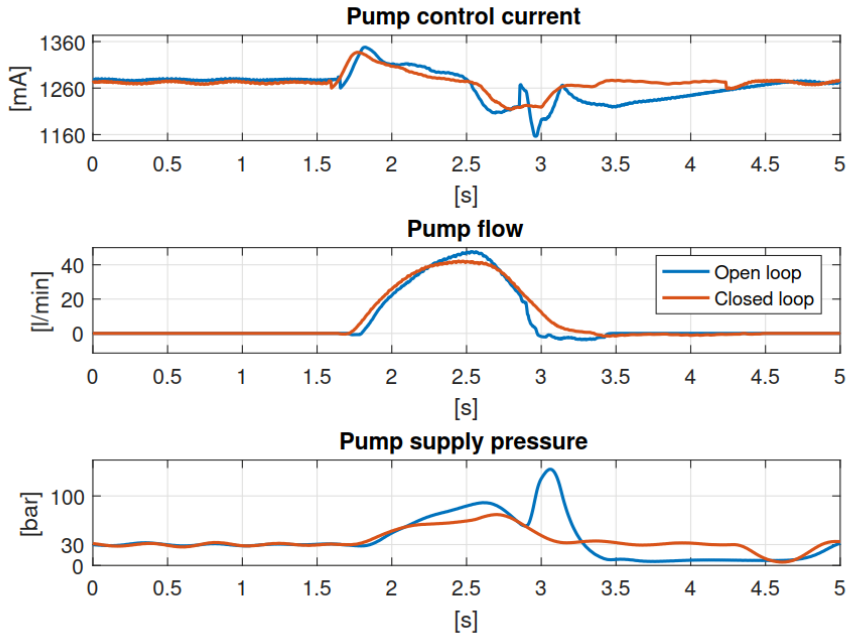


***Figure 8.17.*** *Control signal, which controls the pump as well as flow and pressure provided.*

During both test runs, the reference given by joystick rises above 0.6, which is 60% of the

maximum. Command signal lasts for 1.5 seconds, where as cylinder movement is slightly less.

The signal given to pump is shown in figure 8.17, alongside flow and pressure produced by pump. At 1260 mA pump is at zero position, thus flow into the system is also zero, which can be seen in the figure. Supply pressure is at 30 bar when pressure control is applied, which is before any movement commands. The pump control signal is a bit higher than zero position, when 30 bar supply pressure is maintained due to pump volumetric leakage.

In figure 8.18 tilt valve openings can be seen. When each valve is closed, pressure control mode is acting. In any other case, displacement controller is controlling the flow to the actuators, and in the closed loop case, vibration damping is acting with flow controller.

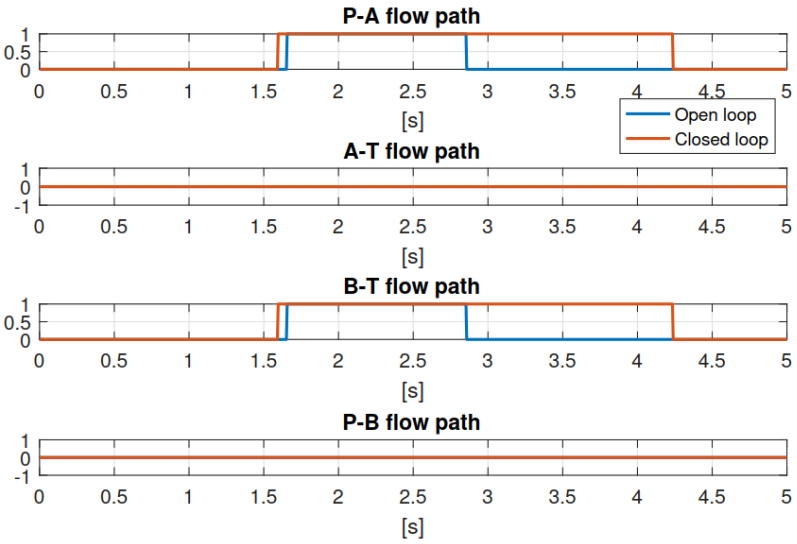


***Figure 8.18.*** *Different flow paths, which control the flow at the tilt cylinder.*

During the open loop test run, the displacement control is active from 1.6 to 2.8 seconds. The starting time can be easily identified from pump control signal in figure 8.17. Also the stopping time is clearly visible in the same graph, where signal makes sudden moves. After the closing moment the supply pressure is swinging heavily, which means there is some room for improvement in gains, which control the stand-by pressure.

Figure 8.18 shows, that during vibration damping mode valves stay open for a 1.5 longer when comparing to the open loop case. In figure 8.17 the pump control current seems to behave much more steadily, and when the closed loop case closes the valves around 4.3 second mark, no such sudden swings can be noted as in open loop case. This can be seen

in supply pressure figure, where no sudden spikes are visible.

Since cylinder pressure in the A chamber is very close to the stand-by pressure of 30 bar as figure 8.19 shows, pump code allows valves to be opened without adjustments to the supply pressure. Cylinder figure shows that pressure in the B chamber is nearly always zero, especially in closed loop case. The pressure in the B chamber rises only when cylinder is moving, which is the pressure difference over the digital valve. This kind of behavior could be eliminated if the valves were operated a bit more intelligent way. Current method, where valves are either open or closed and valve orifice is constant, makes it hard to produced smooth counter pressure in to the chamber.

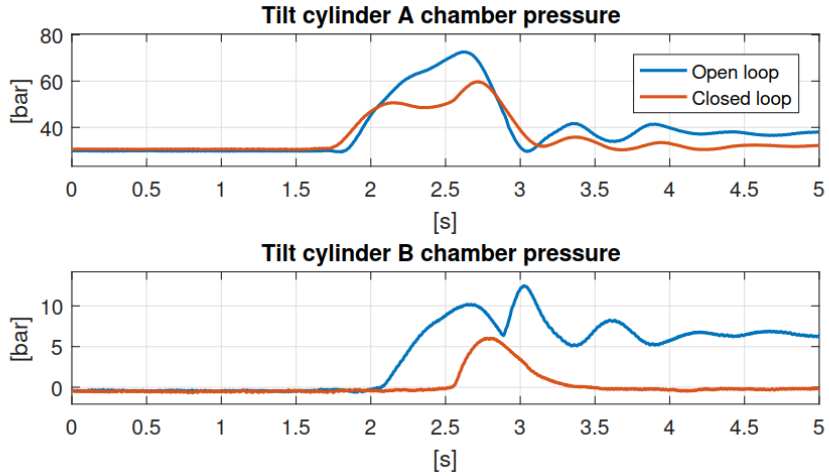


***Figure 8.19.*** *Tilt cylinder chamber pressures during open loop and vibration damping cases.*

Tilt cylinder A chamber pressure shows some signs of damping, since the pressure doesn't rise as high as it does in the open loop case. And this damping can be verified also in figure 8.20, where the acceleration in the tip of the boom is shown. The pressure feedback is clearly reducing the magnitude of the boom vibrations.

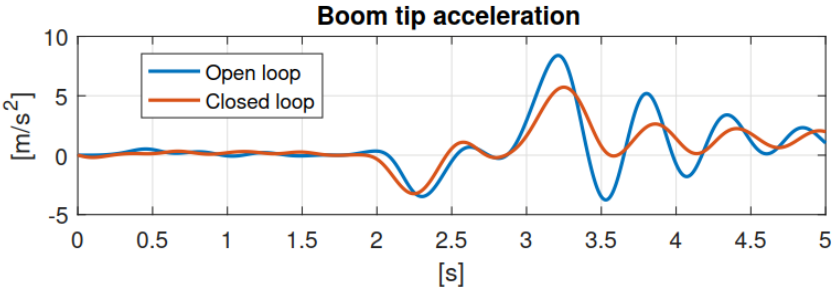


***Figure 8.20.*** *Boom tip acceleration measured with inertial measurement unit.*

Even though the feedback system is able to reduce some of the oscillations of the system, the results are not nearly as good as they where in simulations. Reasons for this may be

the insufficient modeling of vibrations. For example the load fastening to the tip of the boom causes some horizontal vibration to the machine.

### 8.2.2 Lowering the load

In this section the load lowering motion is inspected and discussed more. Since the pump code relies on load mass to generate enough force so it can execute required functions, lifting and lowering are very different cases in that regard.

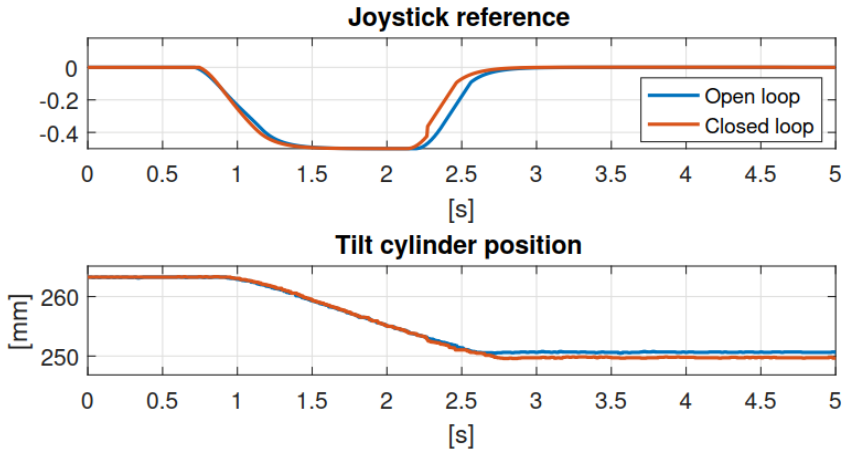


***Figure 8.21.*** *Joystick reference and tilt cylinder position when lowering the load.*

Joystick reference and tilt cylinder position during lowering the load are shown in figure 8.21. Once again, two very similar cases are compared, where other has open loop command, and the other has vibration damping as closed loop controller. Joystick command hits a negative 0.5 magnitude reference as seen in the figure and it lasts approximately 2.7 seconds. Cylinder movement begins at 1 second mark and it stops at 2.7.

In figure 8.22 pump control current, flow and supply pressure are shown. When comparing the control signal given to the pump and flow, it seems the flow saturates during open and closed loop cases. As already mentioned before, this happens because the force that the load mass provides can not generate more flow. After the valves are closed in open loop case as in figure 8.23, the pump swashplate is set to positive angle and yet the flow is negative. Pump control current is slowly ramping up for a second after which the flow turns positive and supply pressure rises. Since the valves are closed, the pressure controller is active. This also seems to refer to the fact that the pressure controller has poor gains.

During vibration damping mode run, the pump pressure doesn't drop to zero as it does in open loop test. As seen in figure 8.23, the valves are open 2 seconds longer, than in open

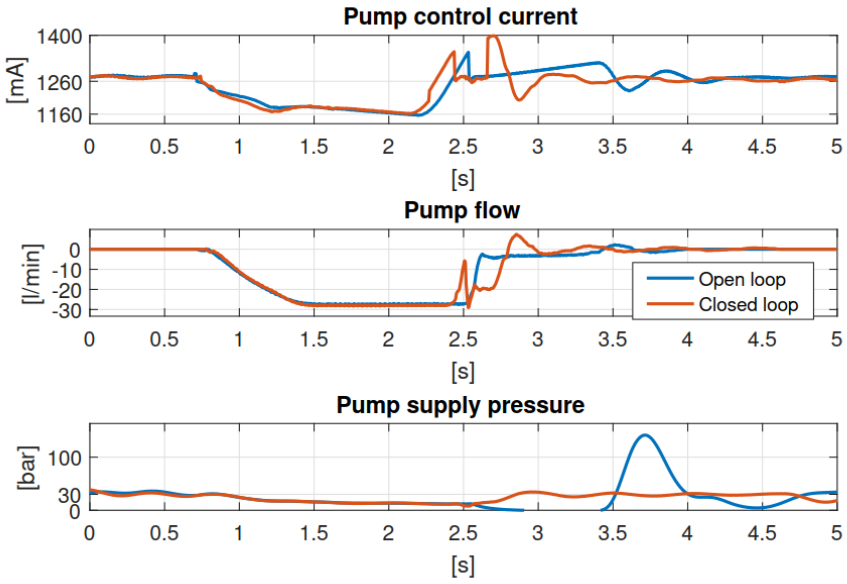


***Figure 8.22.*** *Control signal for the pump, flow and supply pressure when lowering the load.*

loop case. Also a brief moment can be noticed around 2.5 second mark, when valves are shut and then opened again. This is caused by the vibration detection, since it doesn't see any vibrations until the movement stops. Activating the vibration damping means that the pump code enter the displacement control mode.

Figure 8.24 shows the tilt cylinder behavior. The lower chart shows the pressure in the B chamber and it seems to be zero pretty much all the time during the load lowering. A chamber pressure however seems to vibrate during the motion section, which is from 1 to 2.5 seconds. This should trigger the vibration damping feedback and some suppression should be visible in figure 8.25. However, this is not the case, as seen in figure 8.22 the flow saturates, which means small adjustments the pressure feedback would do, doesn't have any effect. After the 2.5 seconds, when the cylinder stops moving and vibration damping is in effect for 2 seconds, nothing really happens when compared to the open loop case.

In the lowering the load case, the vibration damping fails at its task. The major cause to this is the pump code working principle. The flow though the pump saturates, which isn't taken into account when designing the lowering with load mass. Then operator requests more speed, but force generated by gravity has reached its maximum. Therefore pump keeps increasing the angle for nothing, which causes the feedback loop to become ineffective.

Also pressure reaching zero always sounds troubles in hydraulic systems. This easily

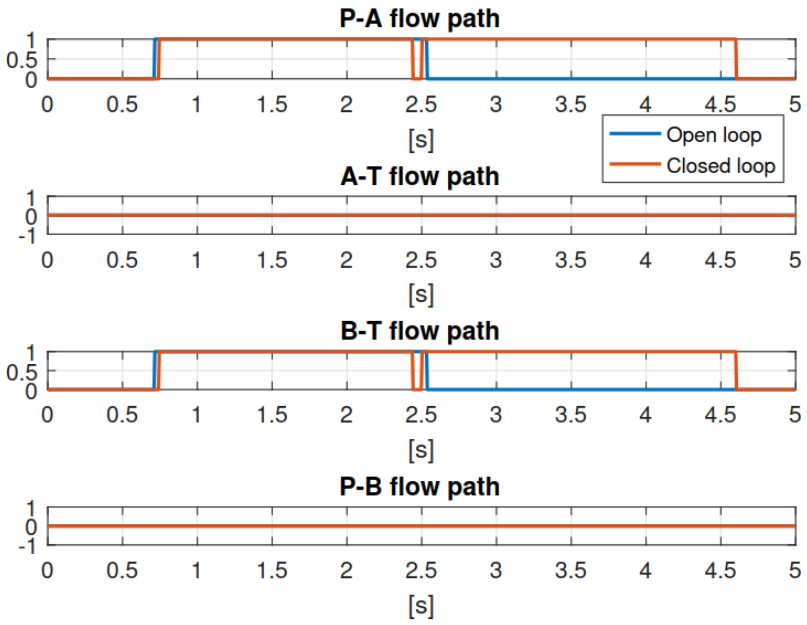


***Figure 8.23.*** *Valve openings when lowering the load.*

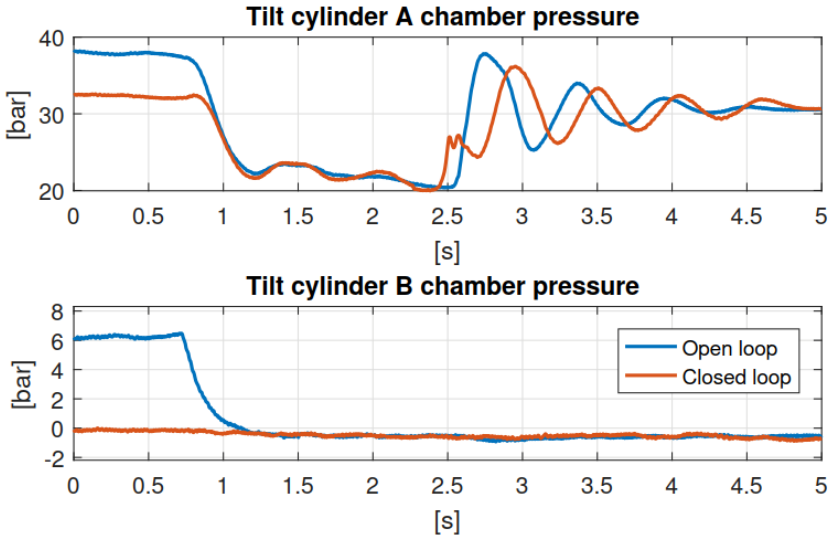


***Figure 8.24.*** *Tilt cylinder pressures in A and B chamber.*

causes cavitation, which then shortens the system lifetime significantly. This type of system, where flow paths are either fully open or closed, doesn't seem to be good as current state. Controlling the flow paths, should be more intelligent to prevent the chamber pressures to reach zero. Since the area of orifice can't be changed, the chamber pressure control would lead to very discrete valve behavior.

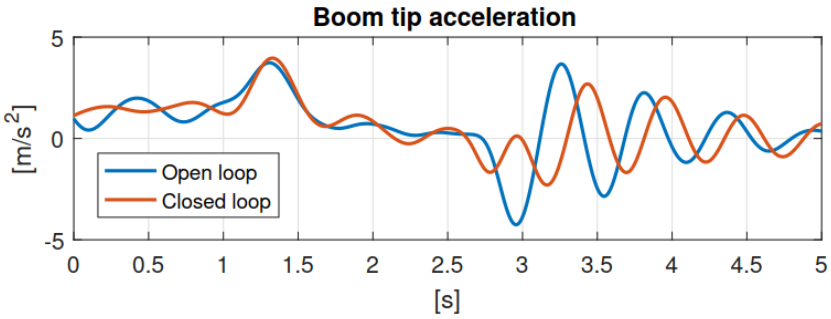


***Figure 8.25.*** *Boom tip acceleration during load lowering.*

If the system would have been driven in a way, where the load had been forced down with pump, meaning that the supply pressure would have been connected to the B side of the cylinder and A side would have been connected to the tank line. It would have increased the velocity of the load significantly, since the high pressure side would have connected directly to the tank, that would have caused the load to the state, where it would nearly free fall. This would also make the vibration damping difficult task.

# 9. FUTURE WORK

In this chapter some ideas, which could be worked with in the future are briefly discussed. While some are mere improvements to the models created during the thesis, others could be described as draft ideas.

During the this thesis, multiple simulator variations were created. Each one of them have common issues, such as long simulation time and poor initial values. One major upgrade for the simulator would be reduction in simulation time, which not only allows more test in same time frame, but also adding a joystick to the system, which could be used to to control the system in a same manner as in the real machine. With better initial values the settling time in the beginning of the simulation could be reduced significantly, or in ideal case eliminated completely.

When using the digital valves and variable displacement pump-motor, pump model doesn't take leakage into account. In reality, this would cause boom to dribble down when valves are open and pump swashplate is at zero position. In simulation this didn't happen, which caused some false assumptions when designing the feedback controller for the system. Also pump model would require a transfer function, which would add some dynamics to describe the pressure compensator and swashplate inertia.

The crane, which acts as a pallet fork extension in the real machine, isn't flexible. Meanwhile the pallet fork itself bends from the root, which causes the whole extension to vibrate. In order to create a situation as in the simulator, a different kind of boom would have been better, such as long aluminum bar.

Even though the pump code was good considering the difficulty of the task, it still has room for improvement. At its current state, the code is flooded with logical operations, which make it complex. Code itself could be transformed into stateflow code, which allows much clearer structural format. Moreover, the controllers could be organized much better as well as their relations.

This experiment also stirred up some related applications, where load pressure could be used to compensate structural vibrations. These could be for example machines where rotational actuators such as motors are used. Trucks, which are used to transport logs,

utilize cranes to manipulate heavy loads same way as forest forwarders. These cranes could benefit same type of load pressure damping as discussed within this thesis, but also implementing same type of vibration suppression system to the crane rotation.

Other systems, which could benefit from vibration damping are applications, that utilize extremely long cranes such as concrete pumps or hoists. These are usually under external forces, which can be wind or in the case of pumps, the method of pumping being very discrete.

During this thesis, the vibration damping was tested with vibrations, which were caused by the operator. Few different kind of scenarios were also discussed where vibration damping could come handy. In addition to those, a case where mobile machine was driven on a rough terrain, was never mentioned, neither tested. Tractors with front loader are often carrying heavy loads, such as water buckets. These could easily expose to oscillations during transportation of bucket full of water.

# 10. CONCLUSIONS

This thesis consisted of testing a pressure feedback control in mobile machines in simulation environment and on real machine. It was previously discovered, that load pressure experienced by cylinder follows the boom bending curvature, which led to a curiosity to test this idea on real machine. At first the goal was to test pressure feedback system in a traditional proportional valve machine, but was changed to digital valve pump controlled system due to availability. Thus multiple different simulators were created to test the performance of the implemented system in proportionally as well as in pump controlled machines. In simulations the boom flexibility was modeled using lumped parameter method, which is sufficient for controller testing purposes. The real machine boom flexibility was created with long crane extension wore over pallet fork, which was bending due to load in the tip of the crane.

Simulation model created was based on Wille urban wheel loader called IHA-machine, which was also used during real machine test phase. There was already a existing model of IHA-machine, created using Simulink Simscape 1st generation multibody functions. This model was recreated using 2nd generation version of Simulink multibody functions, and used in both proportional and digital versions.

Controller design was based on previous experiments, which included analytical solution of two mass spring damper system and Hiab crane simulation. For a proportional valve controlled wheel loader simulation a controller with open loop spool position along with pressure feedback was implemented. Digital valve and pump-motor controlled system used pump control code, which featured displacement and pressure control. The new controlled added vibration damping loop to the displacement control and vibration detection module to valve control section. Controller implemented for simulation was then tested in real machine.

During simulations, the performance of the vibration damping feedback showed promising: in different test scenarios, the controller managed to suppress the oscillations after the initial swing of the boom vibrations. Wheel deflection was also modeled and measured in simulation phase and it also showed damping, meaning the whole machine should remain more stable when boom is driven using vibration damping.

Digital valve model simulation also seemed to be performing well, but when comparing to the real machine, some flaws was encountered. Since pump model didn't take leakage into account, controlled design had few flaws, which were fixed later when the problem was identified. Also lowering the load caused problems, since the force generated by gravity wasn't able to provide enough flow to match the request, leading to unwanted behavior of the controller.

Even though the simulations showed promising, the real machine tests weren't as good as expected. The major cause for this was the experimental pump controlled digital valve system, which still has few issues, even though it is working pretty good considering the very simple idea. The most difficult thing was the valve operation principle, which led to situation, where one flow path from the cylinder was always connected to the tank, whether the motion was positive or negative.

# BIBLIOGRAPHY

[1] *Eaton CMA200 Advanced Sectional Mobile valves*, October 2016.

[2] F. M. Amirouche, *Fundamentals of Multibody Dynamics: Theory and Applications*. Birkhäuser Boston, 2006.

[3] S. Andersson, A. Söderberg, and S. Björklund, "Friction models for sliding dry, boundary and mixed lubricated contacts," *Tribology International*, vol. 40, pp. 580–587, 4 2007.

[4] S. S. Aphale, A. J. Fleming, and S. R. Moheimani, "Integral resonant control of collocated smart structures," *Smart Materials and Structures*, vol. 16, pp. 439–446, 4 2007.

[5] J. Backas, M. Ahopelto, M. Huova, A. Vuohijoki, O. Karhu, R. Ghabcheloo, and K. Huhtala, "Iha-machine: a future mobile machine," in *The twelfth Scandinavian International Conference on Fuild Power, SICFP'11*. Scandinavian International Conference on Fuild Power, May 2011, pp. 161–176.

[6] L. Bascetta and P. Rocco, "End-point vibration sensing of planar flexible manipulators through visual servoing," *Mechatronics*, vol. 16, pp. 221–232, April-May 2006.

[7] J. Becedas, V. Feliu, and H. Sira-Ramirez, "Control of flexible manipulators affected by non-linear friction torque based on the generalized proportional integral concept," in *2007 IEEE International Symposium on Industrial Electronics*, 2007, pp. 12–17.

[8] J. Becedas, V. Feliu, and H. Sira-Ramirezz, "GPI control for a single-link flexible manipulator," in *Proceedings of the World Congress on Engineering and Computer Science*, October 2007.

[9] H. Chaoui, W. Gueaieb, M. C. Yagoub, and P. Sicard, "Hybrid neural fuzzy sliding mode control of flexible-joint manipulators with unknown dynamics," in *IECON 2006 - 32nd Annual Conference on IEEE Industrial Electronics*, November 2006, pp. 4082–4087.

[10] H. Chaoui, P. Sicard, and A. Lakhsasi, "Reference model supervisory loop for neural network based adaptive control of a flexible joint with hard nonlinearities," in *Electrical and Computer Engineering*, vol. 4, November 2004, pp. 2029–2034.

[11] Z. cheng Qiu, J. da Han, X. min Zhang, Y. chao Wang, and Z. wei Wu, "Active vibration control of a flexible beam using a non-collocated acceleration sensor and

piezoelectric patch actuator," *Journal of Sound and Vibration*, vol. 326, pp. 438–455, October 2009.

[12] V. Chudnovsky, A. Mukherjee, J. Wendlandt, and D. Kennedy, "Modeling Flexible Bodies in SimMechanics," White Paper, August 2006.

[13] DeepSoft. FEA element types. [Online]. Available: http://fea-cae-engineering.com/fea-cae-engineering/element_types.htm

[14] X.-J. Dong, G. Meng, and J.-C. Peng, "Vibration control of piezoelectric smart structures based on system identification technique: Numerical simulation and experimental study," *Journal of Sound and Vibration*, vol. 297, pp. 680–693, November 2006.

[15] dSPACE GmbH, *Hardware Installation and Configuration*, March 2005.

[16] G. Dubus, "On-line estimation of time varying capture delay for vision-based vibration control of flexible manipulators deployed in hostile environments," in *IEEE/RSJ International Conference on Intelligent Robots and Systems (IROS)*, October 2010, pp. 3765–3770.

[17] G. Dubus, O. David, and Y. Measson, "A vision-based method for estimating vibrations of a flexible arm using on-line sinusoidal regression," in *IEEE/RSJ International Conference on Intelligent Robots and Systems (IROS)*, July 2010, pp. 4068–4075.

[18] S. K. Dwivedy and P. Eberhard, "Dynamic analysis of flexible manipulators, a literature review," *Mechanism and Machine Theory*, vol. 41, pp. 749–777, July 2006.

[19] V. Feliu, P. Roncero, and J. Lopez, "Repetitive control for single link flexible," in *Proceedings of the 2005 IEEE International Conference on Robotics and Automation*, 2005, pp. 4303–4308.

[20] J. R. Forbes and C. J. Damaren, "Single-link flexible manipulator control accommodating passivity violations: Theory and experiments," *IEEE Transactions on control systems technology*, vol. 20, May 2012.

[21] A. Green and J. Sasiadek, "Inverse dynamics and fuzzy repetitive learning flexible robot control," in *IFAC Proceedings Volumes*, vol. 35, 2002, pp. 139–144.

[22] R. B. Group, *Axial piston variable pump AV10V(S)O Series 31*, June 2016.

[23] H. Heidari, M. Korayem, M. Haghpanahi, and V. Batlle, "Optimal trajectory planning for flexible link manipulators with large deflection using a new displacement

approach," *Jouranl of Intelligent and Robotic Systems*, vol. 72, pp. 287–300, December 2013.

[24] M.-T. Ho and Y.-W. Tu, "Position control of a single-link flexible manipulator using H∞ -based pid control," *IEE Proceedings: Control Theory and Applications*, vol. 153, pp. 615–622, 2006.

[25] H. Karimi and M. Yazdanpanah, "A new modeling approach to single-link flexible manipulator using singular perturbation method," *Electrical Engineering*, vol. 88, pp. 375–382, June 2006.

[26] S. Katsura and K. Ohnishi, "Force servoing by flexible manipulator based on resonance ratio control," *IEEE Transactions on Industrial Electronics*, vol. 54, pp. 539–547, February 2007.

[27] C. Kiang, A. Spowage, and C. Yoong, "Review of control and sensor system of flexible manipulator," *Journal of Intelligent and Robotic Systems*, vol. 77, pp. 187–213, January 2015.

[28] KRACHT GmbH, "Gear type flow meter vc," January 2012.

[29] S. Kuchler, O. Sawodny, K. Schneider, and L. K, "Vibration damping for a hydraulic driven luffing cylinder at a boom crane using feedforward control," *Advanced Intelligent Mechatronics*, pp. 1276–1281, July 2009.

[30] K. Kuo and J. Lin, "Fuzzy logic control for flexible link robot arm by singular perturbation approach," *Applied Soft Computing*, vol. 2, pp. 24–38, August 2002.

[31] J. Lin, Z. Huang, and P. Huang, "An active damping control of robot manipulators with oscillatory bases by singular perturbation approach," *Journal of Sound and Vibration*, vol. 304, pp. 345–360, July 2007.

[32] I. Mahmood, S. Moheimani, and B. Bhikkaji, "Precise tip positioning of a flexible manipulator using resonant control," *IEEE/ASME Transactions on Mechatronics*, vol. 13, pp. 180–186, 2008.

[33] P. Mäkinen, "Modeling and control of a single-link flexible hydraulic robot," Master's thesis, Tampere University of Technology, November 2016.

[34] MathWorks. Finite Element Method (FEM) Basics. [Online]. Available: https://se.mathworks.com/help/pde/ug/basics-of-the-finite-element-method.html

[35] Z. Mohamed, J. Martins, M. Tohki, J. S. da Costa, and M. A. Botto, "Vibration control of a very flexible manipulator system," *Control Engineering Practice*, vol. 13, pp. 267–277, March 2005.

[36] C. Monje, F. Ramos, V. Feliu, and B. Vinagre, "Tip position control of a lightweight flexible manipulator using a fractional order controller," *IET Control Theory and Applications*, vol. 1, pp. 1451–1460, 2007.

[37] E. Pereira, S. S. Aphale, V. Feliu, and S. O. R. Moheimani, "Integral resonant control for vibration damping and precise tip-positioning of a single-link flexible manipulator," *IEEE/ASME Transactions on Mechatronics*, vol. 16, pp. 232–240, 2011.

[38] E. Pereira, S. S. Aphale, V. Feliu, and S. R. Moheimani, "A hybrid control strategy for vibration damping and precise tip-positioning of a single-link flexible manipulator," in *2009 IEEE International Conference on Mechatronics*, 2009, pp. 1–6.

[39] E. Pereira, I. M. Diaz, J. J. Cela, and V. Feliu, "A new design methodology for passivity-based control of single-link flexible manipulators," in *Advanced intelligent mechatronics*, December 2007.

[40] Z. Qiu, "Acceleration sensor based vibration control for flexible robot by using ppf algorithm," in *IEEE International Conference on Control and Automation*, 2007, pp. 1335–1339.

[41] G. G. Rigatos, "Model-based and model-free control of flexible-link robots: A comparison between representative methods," *Applied Mathematical Modelling*, vol. 33, pp. 3906–3925, October 2009.

[42] S. W. Roberts, "Control chart tests based on geometric moving averages," *Technometrics*, vol. 42, pp. 97–101, February 2000.

[43] J.-H. Ryu, D.-S. Kwon, and B. Hannaford, "Control of a flexible manipulator with noncollocated feedback: Time-domain passivity approach," *IEEE Transactions on Robotics*, vol. 20, August 2004.

[44] J. Shan, H.-T. Liu, and D. Sun, "Slewing and vibration control of a single-link flexible manipulator by positive position feedback (ppf)," *Mechatronics*, vol. 15, pp. 487–503, 2005.

[45] G. Song, S. P. Schmidt, and B. N. Agrawal, "Experimental robustness study of positive position feedback control for active vibration suppression," *Journal of Guidance, Control and Dynamics*, vol. 25, pp. 179–182, January 2002.

[46] D. Sun, J. K. Mills, J. Shan, and S. Tso, "A pzt actuator control of a single-link flexible manipulator based on linear velocity feedback and actuator placement," *Mechatronics*, vol. 14, pp. 381–401, 2004.

[47] M. Z. M. Tumari, M. A. Ahmad, M. S. Saealal, M. A. Zawawi, Z. Mohamed, and N. Yusop, "The direct strain feedback with pid control approach for a flexible manipulator: Experimental results," in *11th International Conference on Control, Automation and Systems (ICCAS)*, December 2011, pp. 7–12.

[48] W. Y. Wijaya. (2009, June) FEM Vs. BEM - a comparison in a nut-shell. [Online]. Available: https://willyyanto.wordpress.com/2009/06/14/fem-vs-bem-a-comparison-in-a-nut-shell/